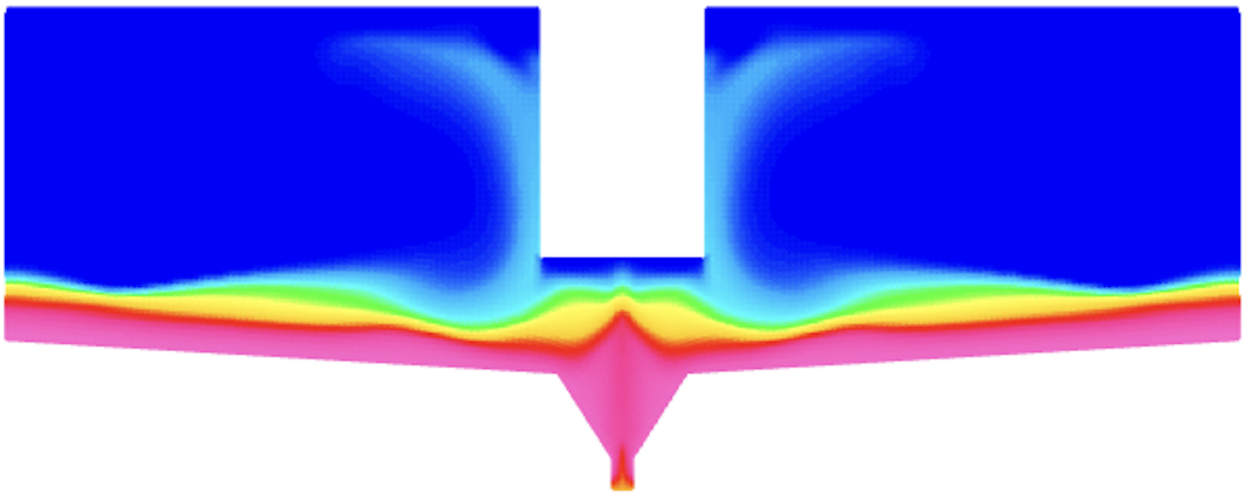

CFD-Driven Optimization of PVC Flocculation and Sedimentation in Industrial Thickener Tank

Enhancing Process Performance and Reducing Environmental Impact

Master's thesis in Sustainable Energy Systems

TILDA LINDQVIST
SIGNE SJÖLIN MARTINSSON

DEPARTMENT OF MECHANICS AND MARITIME SCIENCES
CHALMERS UNIVERSITY OF TECHNOLOGY
Gothenburg, Sweden 2025
www.chalmers.se

Master's Thesis in Sustainable Energy Systems

CFD-Driven Optimization of PVC Flocculation and Sedimentation in Industrial Thickener Tank

Enhancing Process Performance and Reducing Environmental Impact

TILDA LINDQVIST
SIGNE SJÖLIN MARTINSSON

CHALMERS
UNIVERSITY OF TECHNOLOGY

Department of Mechanics and Maritime Sciences
Division of Fluid Dynamics
Chalmers University of Technology
Gothenburg, Sweden 2025

CFD-Driven Optimization of PVC Flocculation and Sedimentation in Industrial Thickener Tank
Enhancing Process Performance and Reducing Environmental Impact
TILDA LINDQVIST
SIGNE SJÖLIN MARTINSSON

Supervisors: Olivia Sandell, INEOS Inovyn
Henrik Ström, Department of Mechanics and Maritime Sciences
Examiner: Henrik Ström, Department of Mechanics and Maritime Sciences

Master's Thesis 2025
Department of Mechanics and Maritime Sciences
Chalmers University of Technology
SE-412 96 Gothenburg
Sweden
Telephone +46 31 772 1000

Cover: Contour plot of the floc product volume fraction during sedimentation in thickener tank.

Typeset in LaTeX
Gothenburg, Sweden 2025

CFD-Driven Optimization of PVC Flocculation and Sedimentation in Industrial Thickener Tank
Enhancing Process Performance and Reducing Environmental Impact
TILDA LINDQVIST
SIGNE SJÖLIN MARTINSSON
Department of Mechanics and Maritime Sciences
Division of Fluid Dynamics
Chalmers University of Technology

Abstract

The aim of the thesis was to optimize the flocculation process of PVC-particles in a thickener tank to increase the separation of microplastics from the industrial drain. This was set to be solved by both testing different flocculation concentrations on-site and by simulating the flow dynamics in ANSYS Fluent. A base model of the tank was developed by calibrating CFD data to match laboratory results. This calibrated model was later used to evaluate the effects of flocculant dosage, PVC inlet concentration and PVC particle size on separation performance. Ultimately, it became clear that particle size was the most critical factor. Fine particles (0.5-1 μm) significantly reduced separation efficiency compared to coarser PVC types (50–250 μm). Additionally, the study identified an optimal PVC inlet concentration (200 mg/L) and flocculant dosage (100 L/h) that minimizes both PVC and flocculant waste.

Keywords: flocculation, CFD, multiphase flow, thickener tank, pvc separation, wastewater treatment

Preface

This report presents the outcome of our master's thesis project carried out at the Department of Mechanics and Maritime Sciences at Chalmers University of Technology during the spring of 2025. The work was conducted in collaboration with INEOS Inovyn and the Division of Fluid Dynamics, as part of the Master's Programme in Sustainable Energy Systems.

Acknowledgements

We would like to express our sincere gratitude to our supervisor and examiner, Professor Henrik Ström, for his invaluable support and guidance throughout this thesis project. His expertise in fluid dynamics and insightful feedback have been crucial to the development and progress of our work.

We would also like to thank our supervisor at INEOS Inovyn, Olivia Sandell, for all of her practical support and valuable assistance. Further we are thankful to Pelle Rönje for explaining the recycling process and showing us around the site, and Helén Axelsson for giving us the opportunity to conduct our thesis at the company.

Additionally, we want to thank Åsa Kaczmarek for letting us analyze the water samples in the laboratory, and Thomas Karlsson and Sonja Colmsjö for teaching us the laboratory methods.

"If you are first in the forest, there is low hanging fruit to pick"

Tilda Lindqvist, Signe Sjölin Martinsson, Gothenburg, May 2025

List of Acronyms

Below is the list of acronyms that have been used throughout this thesis listed in alphabetical order:

CAD – Computer-Aided Design
CFD – Computational Fluid Dynamics
EDC – Ethylene Dichloride
E-PVC – Emulsion-Polyvinyl Chloride
HCl – Hydrochloric Acid
NaCl – Sodium Chloride
NaOH – Sodium Hydroxide
PAC – Polyaluminum Chloride
PAM – Polyacrylamide
PVC – Polyvinyl Chloride
RPM – Rotations per minute
SIMPLE – Semi-Implicit Method for Pressure-Linked Equations
S-PVC – Suspension-Polyvinyl Chloride
VCM – Vinyl Chloride Monomer

Nomenclature

Below is the nomenclature of parameters, variables and indices that have been used throughout this thesis.

A – pre-exponential factor (1/s)
A_{inlet} – cross-sectional area of the inlet (m^2)
C_D – drag force coefficient (–)
C_{NaCl} – NaCl concentration (kg/m^3)
C_{PVC} – PVC concentration (kg/m^3)
D_p – particle diameter (m)
E_a – activation energy (J/mol)
F_k – interphase interactions (N)
g – gravitational acceleration (m/s^2)
g_i – gravitational acceleration component (m/s^2)
k – reaction rate (1/s)
$\dot{m}_{floc}$– mass flow of floc product in outflow (kg/s)
$\dot{m}_{kl}$ – mass exchanged between phase k and l (kg/s)
$\dot{m}_{PVC}$– mass flow of pure PVC in outflow (kg/s)
$\dot{m}_{waste}$– mass flow of total PVC waste in outflow (kg/s)
n – temperature exponent (–)
Q_{feed} – volumetric flow rate of inflow (m^3/s)
$Q_{\text{flocculant}}$ – volumetric flow rate of flocculant (m^3/s)
Q_{outflow} – volumetric flow rate of outflow (m^3/s)
R – universal gas constant (8.314 J/mol · K)
Re – Reynolds number (–)
Re_p – particle Reynolds number (–)
t – time (s)
T – absolute temperature (K)

U – characteristic velocity (m/s)

$U_{i,k}$ – velocity component i in phase k (m/s)

$\vec{u}$ – fluid velocity (m/s)

V_1 – sample volume (m^3)

V_2 – volumetric flask volume (m^3)

v_{feed} – velocity of inflow to tank (m/s)

v_t – terminal velocity (m/s)

$\vec{v}$ – particle velocity (m/s)

x_j – spatial coordinate (m)

$\alpha_{\text{flocculant}}$ – volume fraction of flocculant (–)

α_{floc} – volume fraction of floc product (–)

α_{PVC} – volume fraction of PVC (–)

α_k – volume fraction of phase k (–)

μ_c – dynamic viscosity of carrier fluid ($\text{Pa} \cdot \text{s}$)

ρ_c – density of carrier fluid (kg/m^3)

ρ_k – density of phase k (kg/m^3)

ρ_{PVC} – density of PVC (kg/m^3)

$\tau_{j,k}$ – stress tensor (Pa)

Contents

List of Figures

List of Tables

1
Introduction

A brief overview of the environmental and industrial context of PVC production and wastewater treatment helps clarify the focus of this thesis. The impact of plastic waste, the relevant chemical processes at INEOS Inovyn and the purpose of the thesis are presented below.

1.1 Background

With increasing environmental regulations, industries are required to reduce microplastic emissions from wastewater. At INEOS Inovyn, efforts are focused on improving wastewater treatment efficiency to recover more of produced Polyvinyl Chloride (PVC) and thus minimize environmental impact. This is set to be done by optimizing the existing separation process of the industrial drain.

1.1.1 Impact of Industrial Plastic Waste

Plastics and microplastics enter the ocean through various routes, including direct discharge from chemical plants. Microplastics and associated chemicals have been found in seafood, posing a risk to human health through consumption. These contaminants can cause various health issues, including cancer and endocrine disruption [1] [2]. The degradation of plastics further releases greenhouse gases such as methane and ethylene, contributing to climate change. The presence of plastics disrupts marine ecosystems by altering habitats and facilitating the spread of invasive species, which can lead to a loss of biodiversity and changes in ecosystem functions [1]. The ethical dimension of this issue lies in the responsibility to mitigate harm caused by industrial activities, acknowledging the moral obligation to protect vulnerable ecosystems, prevent human health risks, and address the long-term environmental consequences of plastic pollution and climate change.

1.1.2 INEOS Inovyn

INEOS Inovyn is a leading producer of PVC and operates multiple facilities across Europe, including one of its key production sites in Sweden, Stenungsund. The site manufactures two main types of PVC: Emulsion PVC (E-PVC), which is commonly used in coatings, adhesives, and textiles, and Suspension PVC (S-PVC), which is used for rigid applications such as pipes and profiles.

The production process begins with the manufacturing of vinyl chloride monomer (VCM), a key raw material, which is synthesized from ethylene and chlorine. Apart from PVC, byproducts such as NaOH, HCl and ethylene dichloride (EDC) are sold as products as well.

The PVC production is carried out in batches across several production lines, and the plant also features a dedicated wastewater treatment facility for recovering off-spec PVC. INEOS Inovyn's focus includes minimizing microplastic emissions and optimizing the separation processes in their recycling systems to align with increasing environmental standards. This makes their facilities an important case study for exploring process efficiency and environmental impact in industrial wastewater management.

1.1.3 Wastewater Treatment Facility

The wastewater from production is treated in a facility called PVC Recycling. The goal is to extract as many PVC particles as possible from the wastewater before it flows into the biological treatment plant and the recovered plastic can then be sold as off-spec PVC.

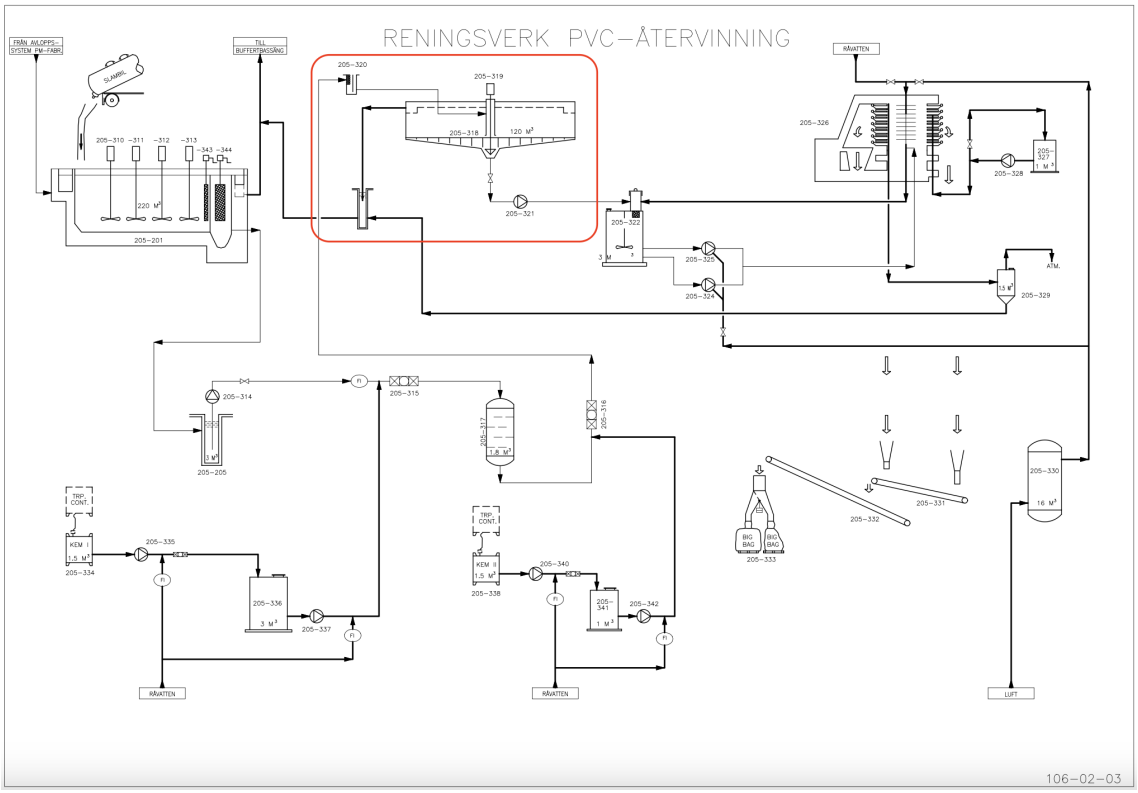

Figure 1.1: PVC recycling process.

The first stage of recycling is the mixing basin, which serves as a buffer tank where pH-adjustments takes place. The wastewater from PVC production contains varying amounts of PVC particles in different sizes, depending on the type of PVC being

produced. From the mixing basin, the water is pumped to the thickener (circled in figure 1.1), a type of sedimentation tank. Here, chemicals are added to the wastewater to promote flocculation. The thickener is designed with an inlet positioned deep within the tank, ensuring that the sludge bed acts as a filter for incoming water. The overflow from the thickener flows to the biological treatment plant, while the sludge at the bottom is transferred to a filter press for further processing.

After the water has been treated in the tank, the overflow still contains an inadequate amount of microplastics. One major factor affecting how much plastic remains after the tank is the flocculation process, which largely depends on the concentrations of added chemicals, the particle size distribution and the hydrodynamics of the flow. However, increasing the flocculant dosage to improve separation comes at a cost, as it leads to higher polymer emissions and increased operational expenses.

1.2 Purpose

The purpose of this thesis is to improve the separation of PVC particles from the industrial wastewater stream at INEOS Inovyn by optimizing the sedimentation process in the thickener tank. The project combines on-site laboratory analyses and theoretical modeling through CFD simulations of the flocculation dynamics, complemented with a literature review of comparable industrial separation processes.

Specifically, the objectives are:

- To quantify the separation efficiency and total PVC waste at different flocculant dosages through laboratory experiments.
- To create and calibrate a CFD model that accurately represents the flow dynamics in the thickener tank when compared to experimental data.
- To investigate the effects of particle size distribution and flow conditions by simulating the flocculation and sedimentation process for different cases using the CFD model.

2
Theory

A broad range of theoretical concepts was needed to understand the industrial separation process, conduct the laboratory experiments and design the CFD simulations. The relevant physical processes, chemical interactions and computational models are presented below.

2.1 Thickener Tank

Thickener tanks are widely used in chemical processes, often to separate solid particles from a surrounding liquid, such as PVC-particles in an industrial drain. The aim of thickener tanks is to separate the inflow into a denser fluid, containing solid particles, by a combination of gravitational forces and a rotating scrape. To increase those forces and thus enhance the separation, the PVC-particles are flocculated with flocculants. The denser phase can then exit at the bottom of the tank. The clear liquid phase is clarified from solid particles and can exit over the edges around the tank [4].

2.2 Chemicals

The chemicals of interest in this thesis are the produced PVC and the flocculating agents that are being used in the water treatment. Flocculation occurs in the process when polyacrylamide and polyaluminium chloride are added to the industrial drain containing PVC.

2.2.1 Polyvinyl Chloride (PVC)

PVC is a widely used synthetic polymer known for its unique chemical properties and versatility in industrial applications. As mentioned, PVC is formed through the polymerization of VCM. This process involves combining ethylene, a byproduct of natural gas, with chlorine derived from the electrolysis of salt. The resulting monomers undergo polymerization, creating long chains of polymers that form PVC in a powder form. This powder is then processed with additives to achieve the desired properties for various applications [3].

One of PVC's standout features is its chemical stability and resistance to degradation. Its strong molecular bonds make it highly durable, allowing it to withstand

harsh environments for decades without significant wear. This property is particularly valued in the construction industry, where PVC is used for pipes, fittings, and insulation. Its resistance to chemicals, including acids and alkalis, also makes it suitable for use in chemical processing equipment and containers [3].

There are, as mentioned before, two main types of PVC, emulsion-PVC and suspension-PVC. Both of these sorts of PVC are always simultaneously produced in several, various types at the site, making it difficult to draw conclusions on how the different particles have affected the industrial drain. The difficulties arise from the two having different physical properties, where E-PVC has a much smaller diameter than the S-PVC. With that said, the size also varies between the different types of emulsion- and suspension-PVC. The smallest produced E-PVC has a diameter of 0.5-1μm m while S-PVC typically has a diameter of 50-250 μm.

2.2.2 Flocculating Agents

Flocculation is a key process in enhancing the separation of PVC particles from industrial wastewater. It promotes the collision of solids and allows them to agglomerate into larger, denser flocs that can then settle in the bottom of the tank [8]. Sedimentation rates are significantly affected by the presence of flocculants; measurements have shown an increase of of 423.5% compared to conditions without chemical additives [13].

In thickeners, this process typically follows a two-step mechanism where one agent first neutralizes particle surface charges of the feed, followed by flocculation through mechanical bridging with a high-molecular-weight polymer. This process is illustrated in figure 2.1.

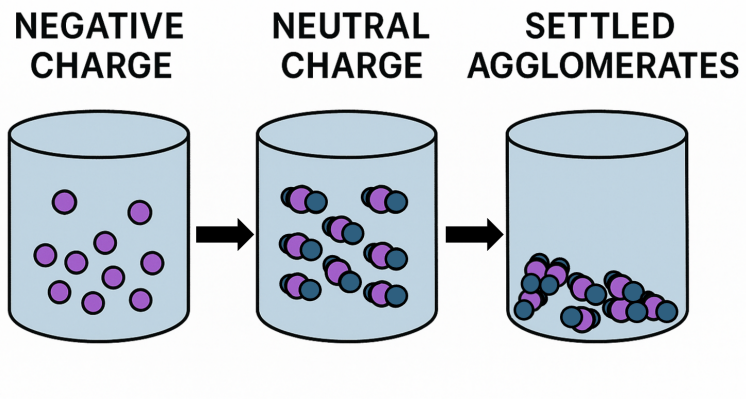

Figure 2.1: Two-step mechanism of flocculation.

2.2.2.1 Polyaluminium Chloride (PAC)

One flocculant used in the process is called ecofloc, which consists of Polyaluminium chloride (PAC) in water. PAC is an inorganic cationic (positively charged) polymeric flocculant widely used in water and wastewater treatment [6]. It consists of

pre-hydrolyzed aluminum species, making it more effective than traditional flocculants like aluminum sulfate. PAC works by neutralizing the negative charges on suspended particles in water, allowing them to form larger flocs, which can then settle and be filtered out.

One of the key advantages of PAC is its high charge density, which enhances flocculation efficiency even at lower dosages compared to conventional aluminum-based flocculants. It is also less pH-dependent, working effectively in a broader pH range, typically between 7 and 9. PAC also generates denser and more compact flocs, improving sedimentation and reducing the amount of residual sludge [6].

2.2.2.2 Polyacrylamide (PAM)

Along with ecofloc, BetzDearborn AE1128 is added. This is a high molecular weight polymer consisting of anionic (negatively charged) polyacrylamide (PAM). It aids in the clarification, thickening, and dewatering processes by forming long molecular chains that bridge between particles, promoting the aggregation of the suspended solids. The chemical is particularly effective in improving sedimentation efficiency when combined with PAC, reducing carryover and enhancing sludge dewatering [7]. Both of these flocculants are pumped into the waste flow from PVC production before it enters the thickener.

2.3 Analytical Chemistry

The concentration of PVC particles in the industrial drain before and after the thickener was analytically determined. This was done by analysing the amount of chloride ions in the water samples in an ion chromatographer.

2.3.1 Ion Chromatography

An ion chromatographer identifies different amounts of cations and anions in a liquid sample. The sample is pumped through a column, which has been filled with negative and positive charged groups. Different ions will bond with different intensity to the column, depending on their properties such as size and affinity. An eluent will then run through the column and the ions will be washed away and exit the column with it. Since the different ions have different bonding properties, they will exit the column and entering the detector at different times, making it possible to determine the amount of wanted ion [5]. When the amount of chloride anion is detected, the concentration of PVC can be estimated in [mg/L].

2.4 CFD Simulation Frameworks

Computational Fluid Dynamics (CFD) is a numerical method for analyzing fluid flow, offering deeper insights than traditional empirical models [11]. Governing equations for mass, momentum, and energy are solved, enabling simulations of multiphase interactions and reactive flows.

The simulation process begins with geometry modelling, where the geometry and its boundaries are defined. This is followed by grid generation, dividing the geometry into small computational cells. Next, appropriate models describing the flow are selected and material properties like density and viscosity are then specified. While single-phase flows can be modelled with high accuracy, multiphase systems such as the PVC separation process require more advanced models for reliable predictions. Boundary conditions are then set before the simulation is solved using the chosen solver settings. Finally, the results are analyzed during the post-processing stage [11].

2.4.1 Multiphase Model

The Eulerian-Eulerian multiphase model describes the statistical behavior of multiphase flow by averaging local properties over space and time [12]. It uses volume fractions to represent the local number of droplets or particles, treating both the dispersed and continuous phases as interpenetrating fluids with closure equations. The model provides average values for volume fraction, velocity, and fluctuations but does not resolve the properties of individual particles or droplets. Each particle is further assumed to geometrically resemble a perfect sphere. It can be derived through volume averaging (which is most relevant for this case), ensemble averaging or probability density functions. The Eulerian-Eulerian model has been used to successfully predict the behavior of many large-scale multiphase flows, such as of fluidized beds and turbulent fluid-particle flows, making it a suitable option for modelling industrial processes [12].

Euler–Euler is derived from the Navier–Stokes equations and adapted to account for the interactions between continuous and dispersed phases. By solving the conservation equations 2.1-2.3 for each phase individually, the model captures momentum exchange, phase volume fractions, and interfacial forces in multiphase flow systems.

$$\sum_k \alpha_k = 1 \tag{2.1}$$

$$\frac{\partial \alpha_k \rho_k}{\partial t} + \frac{\partial \alpha_k \rho_k U_{i,k}}{\partial x_i} = -\sum_{l=1}^{p} (\dot{m}_{kl} - \dot{m}_{lk}) \tag{2.2}$$

$$\frac{\partial \alpha_k \rho_k U_{i,k}}{\partial t} + \frac{\partial \alpha_k \rho_k U_{i,k} U_{j,k}}{\partial x_j} = -\alpha_k \frac{\partial P}{\partial x_i} + \frac{\partial \alpha_k \tau_{j,k}}{\partial x_k} + \alpha_k \rho_k g_i + F_{i,k} \tag{2.3}$$

The constraint in equation 2.1 ensures that the total volume fraction of each phase sums to one. Equation 2.2 accounts for phase mass transfer, where $\dot{m}_{kl}$ represents the mass exchanged between phase k and phase l. The final equation describes the phase momentum, including pressure effects, a stress tensor $\tau_{j,k}$, gravitational forces, and interphase interactions F_k. Solving these equations is numerically challenging due to the need for closure models for interphase forces and stress terms [11].

2.4.2 Chemical Reaction Model

Including chemical reaction modelling in the simulation is essential for describing the flocculation of dispersed PVC particles with the ecofloc and polymer. The reaction kinetics can be defined using the Arrhenius equation, where the reaction rate k depends on temperature and the concentrations of reactants:

$$k = AT^n e^{-\frac{E_a}{RT}} \tag{2.4}$$

where A is the pre-exponential factor, T is the absolute temperature, n is the temperature exponent, E_a is the activation energy and R is the universal gas constant. This allows the software to compute k dynamically during the simulation, depending on the local temperature field. If the energy equation is disabled, ANSYS Fluent assumes a constant temperature, so the T in this equation won't change spatially or over time [17]. The reaction kinetics influence the formation rate of flocs, which in turn affects phase interactions and sedimentation.

The species transport model in Fluent allows definitions of reactions that represent physical or chemical interactions and solve the governing equations for the reacting phases, even if they are not traditional chemical reactions [17]. Since flocculation is a physical aggregation process rather than a strict chemical reaction, simplified stoichiometric ratios are commonly used in CFD modeling to describe the buildup of flocs.

2.4.3 Flow Regime

The flow regime in fluid mechanics is often characterized by the Reynolds number, defined as:

$$\mathrm{Re} = \frac{\rho_c U L}{\mu_c}$$

where ρ_c is the carrier fluid density, U is the characteristic velocity, L is a characteristic length scale, and μ_c is the carrier fluid dynamic viscosity. Flows with $\mathrm{Re} < 2300$ are typically considered laminar, whereas flows with $\mathrm{Re} > 4000$ are considered turbulent, with a transition region in between [11]. For laminar flows, a turbulence model does not have to be applied in the CFD simulation.

The motion of particles in a fluid is governed by Newton's second law, where the total force acting on a particle equals its mass times acceleration [12]. Several forces can act on a particle, such as hydrodynamic drag, lift, buoyancy and gravitational

forces. The drag force depends on the relative velocity between the particle and fluid, which is characterized by the particle Reynolds number:

$$\mathrm{Re}_p = \frac{D_p|\vec{u} - \vec{v}|\rho_c}{\mu_c} \tag{2.5}$$

where D_p is the particle diameter and $\vec{u}$ and $\vec{v}$ are the fluid and particle velocities respectively [12].

Stokes' sedimentation theory describes how spherical particles reach a constant settling velocity based on a balance of all forces acting on them [27]. For small particles in viscous-flow conditions where $\mathrm{Re}_p<1$, the relationship is defined by Stokes' law in equation 2.6.

$$v_t = \frac{(\rho_p - \rho_c)gD_p^2}{18 \cdot \mu_c} \tag{2.6}$$

where v_t is the terminal velocity and g is the gravitational acceleration. As can be seen, the settling velocity is proportional to the square of particle diameter. This means that as the particle size decreases, the settling rate becomes increasingly small.

2.4.4 Drag Force Model

It is convenient to express the steady drag force on particles in terms of a the drag coefficient C_D, which can be modelled in different ways in CFD. The Schiller–Naumann drag model is an empirical correlation used to calculate the drag force between the fluid and dispersed particles. The drag coefficient C_D is defined as a function of the particle Reynolds number Re_p, according to the following expression:

$$C_D = \begin{cases} \frac{24}{\mathrm{Re}_p}\left(1 + 0.15\,\mathrm{Re}_p^{0.687}\right), & \mathrm{Re}_p < 1000 \\ 0.44, & \mathrm{Re}_p \geq 1000 \end{cases}$$

This correlation is applied within the drag force term of the Euler–Euler multiphase model to describe momentum exchange between the continuous and dispersed phases. It is suitable for spherical particles and is widely used in dense particle suspensions [14].

The Morsi–Alexander drag model is an empirical correlation that instead expresses C_D as a polynomial function of the particle Reynolds number Re_p. Unlike simpler correlations, it introduces a piecewise formulation with different coefficients depending on the Reynolds number range:

$$C_D = \frac{A}{\mathrm{Re}_p} + \frac{B}{\sqrt{\mathrm{Re}_p}} + C$$

The constants A, B, and C vary depending on the value of Re_p, allowing the model to account for a wider range of flow conditions. This makes it suitable for use in

systems with varying particle sizes and flow regimes. The model was originally developed based on experimental data for spherical particles in uniform flow [14].

2.4.5 Discretization and Coupling

Upwind schemes are numerical methods where the face values depend only on upstream conditions. In the first-order upwind scheme, the face value between two cells is simply set equal to the value in the nearest upstream cell, ensuring physical reliability for convective flows. This approach works well when convection dominates and the flow is aligned with the grid. It is bounded and robust at a low computational cost. However, it may introduce numerical diffusion and can be replaced by higher-order schemes for higher accuracy [11].

Pressure-velocity coupling ensures an accurate simulation of fluid flow by linking pressure and velocity fields. This coupling is essential for solving the Navier-Stokes equations, which describe the motion of fluid substances. The SIMPLE (Semi-Implicit Method for Pressure-Linked Equations) algorithm is a widely used method that is known for its robustness and simplicity. The algorithm operates by guessing a pressure field, solving the momentum equations to compute velocity fields, and then correcting the pressure and velocity fields iteratively to satisfy the continuity equation [19].

3
Literature Study

To identify effective strategies for improving PVC separation, relevant findings from previous studies have been reviewed. The literature covers optimal mixing conditions, chemical dosing strategies, particle size effects and operational challenges such as floc bed formation.

3.1 Optimal Mixing and Chemical Dosing

The American Water Works Associasion identified optimal mixing conditions for microplastic removal on a laboratory scale using a two-step stirring protocol: an initial rapid stirring phase at 240 rpm for 1 minute, followed by slow stirring at 35 rpm for 13 minutes [23]. In this experiment, the water was combined with 0.4 mmol/L PAC and 3 mg/L PAM at pH 8. This treatment setup achieved removal efficiencies above 95% for various microplastic types, including PVC. The results highlight the importance of sufficient initial mixing to ensure proper flocculant dispersion and effective particle aggregation prior to sedimentation, and confirm that PAM and PAC is an optimal combination of flocculants.

A study from the Journal of Central South University further confirms that it is optimal to apply a dual flocculation process, as using the advantages of two polymers enables different flocculation mechanisms to operate in sequence [24]. Optimal results were found using one anionic and one cationic polymer, as the anionic flocculant captures fine particles (<100 μm) while the cationic flocculant promotes regrowth of broken flocs via charge neutralization. Together, they effectively trap fine particles and form large, stable flocs. Important to note however, is that the finest produced particles in the thickener tank are still significantly smaller than 100 μm.

3.2 Optimal PVC Inlet Concentration

From a study on thickeners in the Gol-e-Gohar iron ore complex in Iran, diluting the feed to the tank was found to significantly enhance flocculation [16]. The tanks were consuming too much flocculant simoltaneously as the recycled water had large amounts of suspended solids, and it was found that the high solid content of the feed was one of the issues due to the low weight recovery of fresh feed. A diluting pump was installed to decrease the average solid content of the feeds by 5%, which hade huge effects. The required flocculant dosage decreased by 65% and the previously problematic thickener overflow was clear and contained <250 ppm of waste [16].

3.3 Particle Size Effect on Flocculation

Particle size has a clear impact on separation efficiency. A study on enhancing microplastic removal from natural water demonstrated that larger microplastic particles (250μm to 1 mm) were removed with an efficiency of up to 95%, whereas smaller particles (<250μm) showed significantly lower removal rates, around only 49% [23] . Another study on particle size measurements for monitoring flocculation responses showed that even finer particles (<20 μm) reduce flocculation efficiency significantly in thickener tanks [15]. Although coarse particles dominate volume-based measurements, it is the fine particles that govern surface area and reactivity with flocculants. Slurries with a high fraction of very fine particles required significantly higher flocculant dosages and often dilution to achieve acceptable settling. The study highlights how many flows actually flocculate well at the correct solids concentration for the correct particle size. However, there are physical limitations on what can be achieved to optimize each of these things simultaneously.

These studies indicate that an increasing fines content in the inflow of the tank negatively affects settling flux, while coarser particle distributions lead to more efficient flocculation at lower dosages [15]. The findings underline the importance of understanding the particle size distribution of the feed when optimizing the chemical dosing and solids concentration, and perhaps mixing in more coarse particles into the fine feeds could help.

3.4 Floc Bed Formation

A floc bed builds up at the bottom of the thickener, consisting of a fluidized zone and a compression zone. As particles agglomerate and settle, the rotating scrape promotes thickening and the underflow maintains an equilibrium in the system. If a thickener does not preserve a mass balance (input – output = accumulation), an excessive floc bed buildup can occur. This can lead to required shutdowns and manual cleanouts. When solids accumulate too much at the bottom of the tank, solids may overflow, underflow may become too dense to pump and a “doughnut” can form which reduces separation. Further, the rotating scrape may overload and stop. Coarse particles especially increase the torque load on the scrape as they rapidly raise mechanical stress in the system [26]. To avoid these issues, bed pressure, density and size distribution of the feed, torque and position of the scrape may be adjusted. The intensity of turbulence within the thickener also affects the collision and aggregation of particles, as high turbulence can lead to the formation of larger flocs that settle quickly and form a dense bed [25].

4

Laboratory Analysis

In order to practically evaluate the flocculation process in the thickener, water samples were collected from the inlet and outlet of the tank after adjusting the dosage of ecofloc and polymer. The PVC concentration in the samples was analyzed to assess separation efficiency, complemented by visual observations and photographs. Operational parameters such as flow rate and the type of PVC produced were recorded as they influence particle behavior. The procedure was repeated with different chemical dosages to optimize floc formation.

4.1 Calibration of Dosage Pumps

Before starting the laborative work, the pumps delivering ecofloc and polymer to the thickener tank needed to be calibrated in order to enable measurements of what chemical dosage they provided the feed with.

The ecofloc pump is flow compensated, meaning that the added concentration remains proportional to the total water flow, which varies over time. The polymer pump, on the other hand, delivers a fixed dosage [L/h] regardless of the flow rate. This causes the effective polymer volume fraction to vary slightly depending on the current water flow.

4.2 Collection of Samples

Water samples were collected both upstream and downstream of the thickener tank. Before sampling, the dosage of ecofloc or polymer was adjusted manually by regulating the flow rate of their respective dosage pumps. Samples were taken after allowing the system to stabilize under the new conditions for about 24 hours. At least three samples were taken for each concentration case. The upstream sample was collected from the mixing basin (basin 205-201 in figure 1.1), while the outlet sample was taken from the thickener tank overflow. At each sampling point, relevant process data such as the instantaneous flow rate and the type of PVC produced were noted, as these parameters influence particle characteristics and sedimentation behavior.

In addition to concentration measurements, visual observations of the water clarity and the appearance of flocs were documented through photographs. The sampling

and analysis procedure was repeated for different dosing conditions in order to evaluate the optimal ecofloc and polymer concentrations for efficient separation.

4.3 Analysis of PVC Concentration

To determine the concentration of suspended PVC particles in the collected wastewater, water samples were filtered, processed and analyzed using ion chromatography.

A defined volume (10–250 mL) of wastewater was filtered through a 1.2 µm Millipore filter to capture suspended solids, by letting at least 1 mg of material remain on the filter. The filter was then rinsed with deionized water to remove chloride residues and dried at 105°C for one hour. After drying, the filter paper was placed in a Schoeniger flask and 15 mL of deionized water was added. The dried filter paper was then wrapped in combustion paper and secured in a platinum holder. The Schoeniger flask was subsequently filled with oxygen before ignition of the combustion paper. The complete combustion process was conducted while tilting the flask to protect the platinum components and ensure full oxidation, as shown in figure 4.1.

Following combustion, the flask was swirled to dissolve all combustion residues into the water. After cooling, the liquid was transferred to a 50 mL volumetric flask and further diluted to a level suitable for analysis. The sample was then analyzed using a Metrohm 930 Compact IC Flex ion chromatographer, depicted in figure 4.2. The autosampler was prepared, and the analysis was conducted using the NaCl-NaBr-Na_2SO_4 calibration method, with a 7-point calibration curve ensuring accurate quantification.

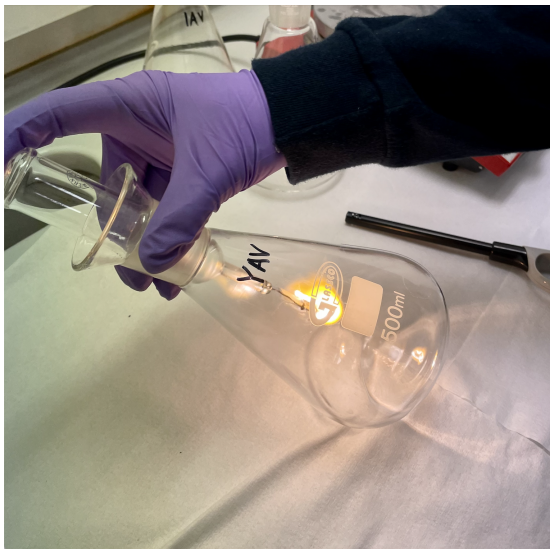

Figure 4.1: Combustion process.

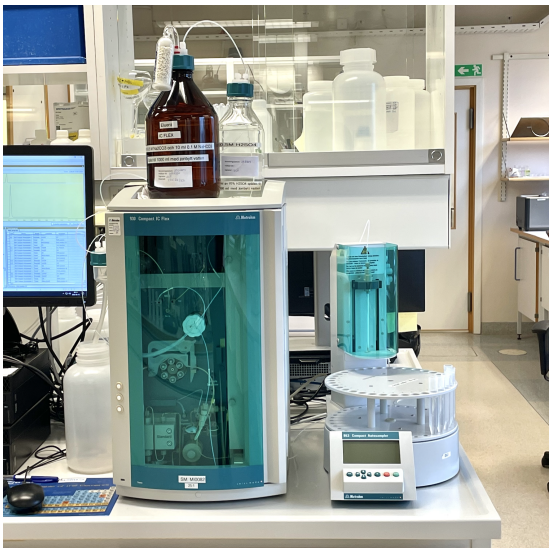

Figure 4.2: Ion chromatograph.

The ion concentration was converted to PVC concentration using a pre-determined conversion factor of 1.07, where the result in mg NaCl/L was recalculated to mg

PVC/L based on the established relation between NaCl and PVC content. The PVC concentration was calculated using the following equation,

$$\mathrm{C}_{PVC} = \frac{\mathrm{C}_{NaCl} \times 1.07 \times V_2}{V_1} \tag{4.1}$$

where C_{PVC} is the PVC concentration, C_{NaCl} is the resultant NaCl concentration, 1.07 is the conversion factor from NaCl to PVC, V_1 is the sample volume and V_2 is the volumetric flask volume. The complete separation of PVC was then calculated accordingly:

$$\%\text{-separation} = \left(1 - \frac{\mathrm{C}_{\mathrm{PVC,outlet}}}{\mathrm{C}_{\mathrm{PVC,inlet}}}\right) \times 100 \tag{4.2}$$

To find the total PVC waste in the water in [mg/h], the concentration was multiplied with the outlet flow rate using the following formula.

$$\dot{m}_{waste} = C_{PVC} \times Q_{outflow} \tag{4.3}$$

where $Q_{outflow}$ was on average 79000 l/h. Tests were carried out on at least two different samples for each polymer - and ecofloc dosage level respectively, in order to account for other influencing parameters such as produced kind of PVC and flow rate.

5

CFD Simulation

CFD simulations of the tank dynamics were conducted to capture the interaction between water, suspended PVC particles, added chemicals and formed flocs under varying conditions. Initial estimates of reaction parameters and material properties were used to define a first version of the model, referred to here as the baseline setup. These values served as a starting point for further refinement in the model calibration section, to obtain more realistic flocculation behaviour and separation performance.

5.1 Geometry and Meshing

The CAD model of the tank geometry was drawn in ANSYS DesignModeler and was based on the sketch of the tank, showcased in figure 5.1. The full CAD model is shown in Appendix A in figure A.1.

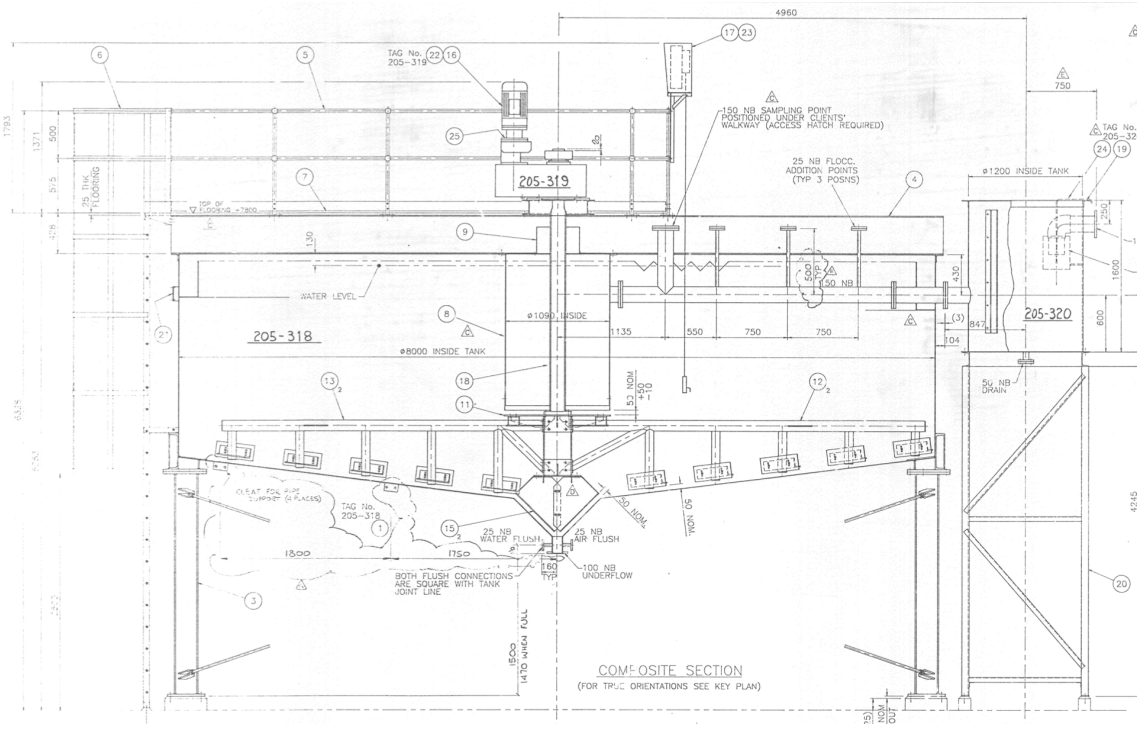

Figure 5.1: Sketch of the thickener tank.

A 2D-axisymmetric rendition of the tank was made in order to cut down on computational costs, while still maintaining a high accuracy considering the tank is axisymmetric in reality. However, this decision meant neglecting the effects of the rotating scrape. This was done since the rotational effects were deemed insignificant as the rotating speed was only 0.16 RPM, but other effects from the scrape that may be present were not accounted for in the simulations.

The generated mesh displayed in figure 5.2 was constructed with the guidelines listed in table 5.1 in mind. To acheive a sufficient mesh quality, the shape used was tetrahedral, the element size was set to 0.8 and refinement was applied to the whole domain, resulting in 5251 cells.

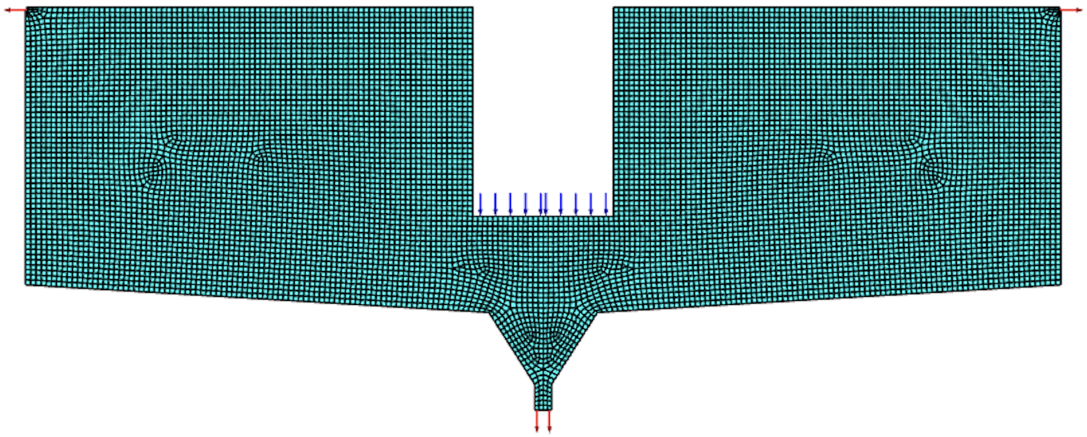

Figure 5.2: Generated mesh.

Table 5.1: Mesh quality evaluation.

Metric	Value	Recommended
Aspect ratio	< 3.64240	< 5
Skewness	< 0.60215	< 0.94
Orthogonal quality	> 0.69837	> 0.15

Table 5.1 shows an evaluation of the mesh that reaches recommended values [11] [21].

5.2 Physical Models

The simulations were conducted using the Euler–Euler multiphase model, with each material being described as a separate phase. Chemical reactions were enabled using the species transport model, with a reaction defined between PVC and the added chemicals to form a separate floc product phase. The ecofloc and polymer were combined into a single species, hereonafter referred to as just "flocculant", to reduce model complexity as both components are added simultaneously and act together in

the flocculation process. Since simplified stoichiometric ratios are commonly used to model physical aggregation processes, the reaction was defined to follow the form:

$$50A + 50B \rightarrow C \tag{5.1}$$

where A represents PVC particles, B is the added chemicals (flocculant and polymer), and C is the resulting floc. The use of equal stoichiometric coefficients (50:50) reflects that both components are required in significant quantities to form a stable floc, rather than assuming that a single reactant would dominate the process.

In the Arrhenius equation 2.4, the pre-exponential factor and activation energy values were estimated from literature [22]. The temperature exponent was set assuming no significant dependence, and Fluent's default normalization temperature was applied. The kick-off temperature of was selected to ensure that the reaction is active throughout the tank. The values listed in table 5.2 were applied for the baseline setup, and later altered in the model calibraton.

Table 5.2: Arrhenius reaction parameters used in the simulation.

Parameter	**Value**
Pre-exponential factor [1/s]	1.0×10^5
Activation energy [J/mol]	1.0×10^4
Temperature exponent	0
Normalization temperature [K]	1
Kick-off temperature [K]	293

Thermal effects such as heat transfer or temperature-dependent behavior do not need to be solved for as the temperature throughout the tank is constant, therefore the energy equation was disabled in the simulation settings.

Although the Reynolds number right by the inlet suggests slightly turbulent conditions, the flow rapidly decelerates directly after entering the tank due to the large cross-sectional area and low overall flow energy. No turbulence model was applied since the flow is laminar in nearly all regions of the tank and the main focus is the laminar settling of flocs.

For phase interactions, the Schiller–Naumann drag law was used to model momentum exchange between the continuous phase and each dispersed phase, as it is well-suited for spherical particles in Newtonian fluids at moderate Reynolds numbers, with the value for Re_p being $\ll 1000$. Between the PVC particles and formed flocs, the Morsi-Alexander drag model was applied to account for varying particle sizes. Lift forces and virtual mass effects were not included in the simulations, since their influence on flocculation was considered negligible due to the low relative velocities and laminar flow regime. Interphase mass transfer was only accounted for in the form of chemical reactions between species and not as physical transfer between phases.

5.3 Material Properties

Water properties were taken from literature [20], while other phase properties were estimated due to a lack of detailed data. The values displayed in table 5.3 were implemented as an initial estimate, and later altered in the model calibration.

Table 5.3: Material properties used for the different phases in the CFD model.

Property	PVC	Flocculant	Floc Product	Water
Diameter [m]	0.0005	0.00001	0.005	-
Density [kg/m^3]	1300	1100	1200	998.2
Viscosity [kg/ms]	0.001003	0.001003	0.001003	0.001003
Molar mass [g/mol]	100000	1000000	1000000	18.0152

Diameters for PVC and formed flocs were based on production data and visual observations. The flocculant is added as a dilute polymer solution in which individual polymer molecules are dissolved rather than existing as distinct solid particles, so assigning a physical diameter this phase is not straightforward. To enable multiphase modeling in Fluent, a representative diameter of 10 μm was assumed based on literature describing the hydrodynamic size of polymer solutions [18]. This value does not represent an actual particle size, but rather serves as a transport scale for drag and interaction modeling.

Similarly, densities of added chemicals and PVC were estimated from theoretical data for similar chemicals, and for the floc product their average value was applied [9] [10]. Since all materials are dispersed in water and present at low concentrations, the overall flow behaves similarly to a water-based fluid which has a constant viscosity. Thus, a viscosity equal to that of water was used for all phases.

Since the reactants consist of long chains of repeating units, their molar masses vary with polymerization degree. A representative molar mass was assumed for PVC based on typical values in industrial literature [8]. For the flocculant and polymer, a molar mass which lies within the typical range for high molecular weight water treatment polymers [7] was used, and the same was applied for the floc product.

5.4 Numerical Setup

Boundary conditions were defined based on the physical configuration of the tank. A velocity inlet was applied to match the experimental flow rate, with the baseline velocity calculated as

$$v_{feed} = Q_{feed} \times A_{inlet} \tag{5.2}$$

where Q is the volumetric flow rate and A is the cross-sectional area of the inlet. Volume fractions at the inlet were calculated based on the average concentrations and flow rates, with the following equations:

$$\alpha_{PVC} = \frac{Q_{feed} \cdot C_{PVC}}{\rho_{PVC}}, \quad \alpha_{flocculant} = \frac{Q_{feed}}{Q_{flocculant}} \tag{5.3}$$

where α is the volume fraction, Q is the volumetric flow rate, C is the concentration and ρ is the density.

Outflow outlets were applied at both the top and bottom of the tank. The division of massflow was specified at the water - and PVC outlets with fractions of 0.9875 and 0.0125 respectively from flow data. No-slip conditions were applied at the tank walls, while a free-slip boundary was used for the water surface. The temperature throughout the whole process was held constant at 308K.

In order to reflect the realistic conditions inside the thickener tank, an initial bed of floc product with a volume fraction of 0.4 was patched at the bottom of the tank domain. This layer represents the settled flocs that accumulate during operation and are influencing both sedimentation and flow distribution.

The simulation was run in transient mode, as both flocculation and sedimentation are time-dependent processes. A steady-state assumption would not be suitable, since it would fail to capture the gradual formation of flocs and the development of dynamic concentration gradients throughout the tank. A first order upwind numerical scheme was applied to decrease computational cost, and the SIMPLE algorithm was used for pressure–velocity coupling. To ensure adequate temporal resolution and numerical stability, a fixed time step of 0.01 s was used. Under-relaxation factors were set to 0.3 for pressure and momentum, and 0.2 for volume fractions, following recommended values for multiphase stability in Fluent [17].

Convergence was monitored through residuals for continuity, momentum and volume fraction. Solutions were considered converged when no further changes were observed in outlet concentrations and volume fraction distributions. The convergence criteria was set to 0.0001. Further, mass balance was monitored to ensure the physical validity of the solution.

5.5 Model Calibration

To ensure that the simulation model reflected the physical behaviour observed in the real system, an iterative calibration process was carried out for uncertain parameter values. Further, a grid independence study was conducted in order to determine whether the mesh was sufficient.

5.5.1 Iteration Cases

Starting from the baseline setup, uncertain parameters were adjusted and tested. Each simulation was evaluated based on whether flocculation occurred as expected and whether the separation efficiency was accurate. This evaluation was enabled

since the separation efficiency could be compared to the laborative results. The new, refined model then served as the foundation for the following case studies.

Table 5.4: Parameter values tested during model calibration.

Parameter	Initial Value	Tested Range	Final Value
Stoichiometry	50A+50B	40A+50B, 50A+40B, 100A+50B, 50A+50B	50A+50B
Floc diameter [m]	0.00001	0.001-0.000001	0.00001
PVC volume fraction	0.0000769	0.0000769-0.0001154	0.0001154
Floc bed volume fraction	0	0-0.5	0.4
Pre-exponential factor [1/s]	100000	100-1000000	1000000

Table 5.4 summarizes the parameters with high uncertainty that were tested based on the baseline setup. Each parameter was tested within a reasonable range based on literature or process data. The final value was selected based on agreement with laboratory results and simulation stability.

5.5.2 Mesh Sensitivity Analysis

To assess the appropriate mesh density for achieving grid-independent results, two new grid variations were evaluated along with the original with 5251 cells. Refined Mesh 1 had 10213 cells and was refined in regions of very high PVC volume fraction gradients shown in figure 5.3. Refined Mesh 2 had 16069 cells and was refined in all zones where PVC volume fraction gradients were moderately high shown in figure 5.4. Each grid satisfied the criteria listed in table 5.1.

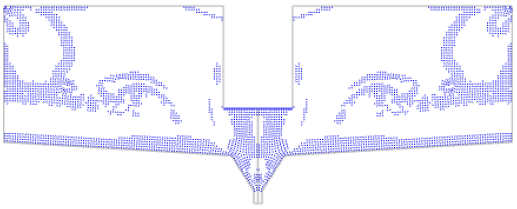

Figure 5.3: Grid adaption zone used for Refined Mesh 1.

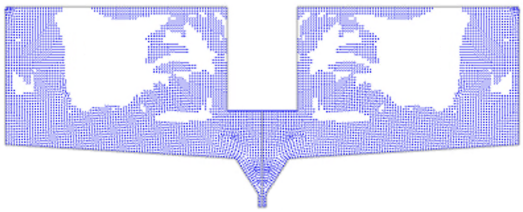

Figure 5.4: Grid adaption zone used for Refined Mesh 2.

For each mesh, the variation in PVC volume fraction in the water outlet during the first few seconds right before converging was tracked using the calibrated model. Results were then plotted in figure 5.5 for comparison.

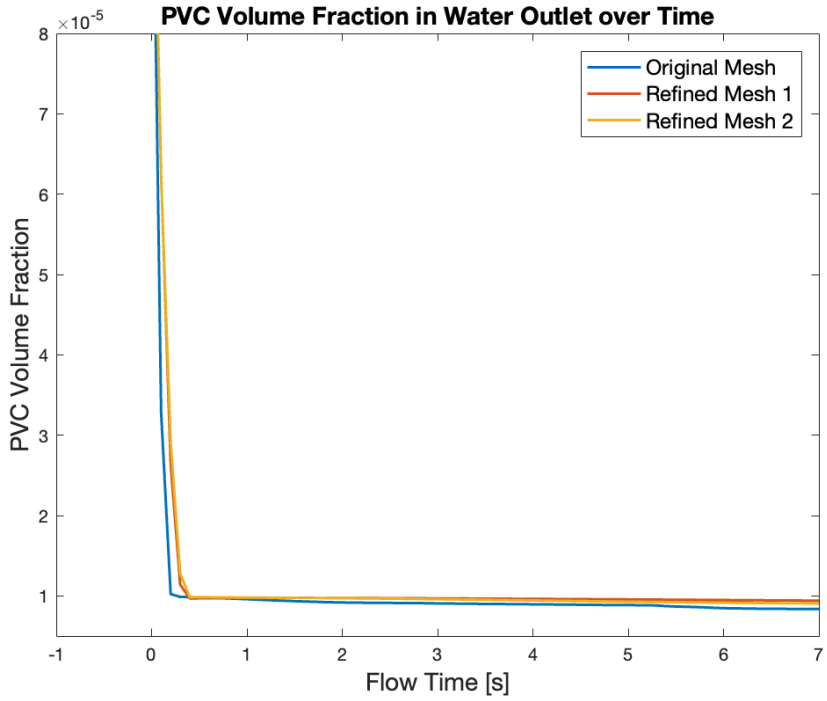

Figure 5.5: Comparison in performance between the three meshes.

It is clear that the three meshes provided very similar results. Although the two refined meshes showed closer agreement with each other than the original, these deviations were considered negligible. Monitors of outlet concentrations of flocculant and floc product were analyzed as well, but no difference could be seen for the three meshes. Therefore the original mesh was retained to reduce computational cost without compromising accuracy.

5.6 Simulation Cases

Simulations were conducted using the calibrated CFD model for varying inlet dosages of both flocculant and PVC, and for different particle sizes of PVC in the following cases.

The first simulation was that of the calibrated model, which was perfected to showcase flocculation, sedimentation and separation as realistically as possible, with average values applied for the fluctuating parmeters. Separation of PVC, flocculant consumption and total waste in [g/h] were evaluated from surface integrals by the water outlet, using the following equations.

$$\%\text{-separation} = \left(1 - \frac{\alpha_{\text{PVC,outlet}} + \alpha_{\text{floc,outlet}}}{\alpha_{\text{PVC,inlet}}}\right) \times 100 \tag{5.4}$$

$$\%\text{-consumption} = \left(1 - \frac{\alpha_{\text{flocculant,outlet}}}{\alpha_{\text{flocculant,inlet}}}\right) \times 100 \tag{5.5}$$

$$\dot{m}_{waste} = \dot{m}_{PVC} + \dot{m}_{floc} \tag{5.6}$$

Each of the parameter studies that were carried out following the original case are listed below:

- A **Chemical Dosage Study** was conducted in order to complement the laborative work. The effect of different inlet flocculant concentrations was investigated with the goal of determening the minimum required amount. Tested volume fractions ranged from 0.00001-0.01, which corresponds to dosages of 0.8-800 L/h. Separation, total PVC waste and flocculant consumption were calculated using equations 5.4-5.6.

- A **PVC Particle Size Study** was conducted, where the effect of the different produced S-PVC and E-PVC types was investigated, also as a way of complementing the laborative work. Tested diameters ranged from 0.005 μm - 500μm, where the size of floc product was always assumed to be larger by a factor of 100. Separation and total PVC waste were calculated using equations 5.4 and 5.6.

- A **PVC Production Study** was conducted, where the effect of different PVC inlet concentrations was investigated, since this also varies on-site and studies suggested dilution of the flow can improve separation efficiency. Tested concentrations ranged from 15-1000 mg/l, which was translated to volume fractions using equation 5.3. These corresponded to a volume fraction range of 0.00001155-0.00076923. Separation, total PVC waste and flocculant consumption were calculated using equations 5.4-5.6.

6
Results and Discussion

The results from both the laboratory expermients and the simulations are presented below. This combination approach enabled both validation of the CFD model against real data and prediction of new operational scenarios.

6.1 Laborative results

The results obtained from the laborative analyses are showcased below for different dosages of polymer, ecofloc and varying PVC particle sizes.

6.1.1 Polymer Dosage

When logging the data from the exact times the samples were taken, it was clear that only the standard sized particles are being produced most of the time. This meant that the results included for the dosage-studies were those obtained for the days the larger kinds of PVC were being made, as there was enough data points.

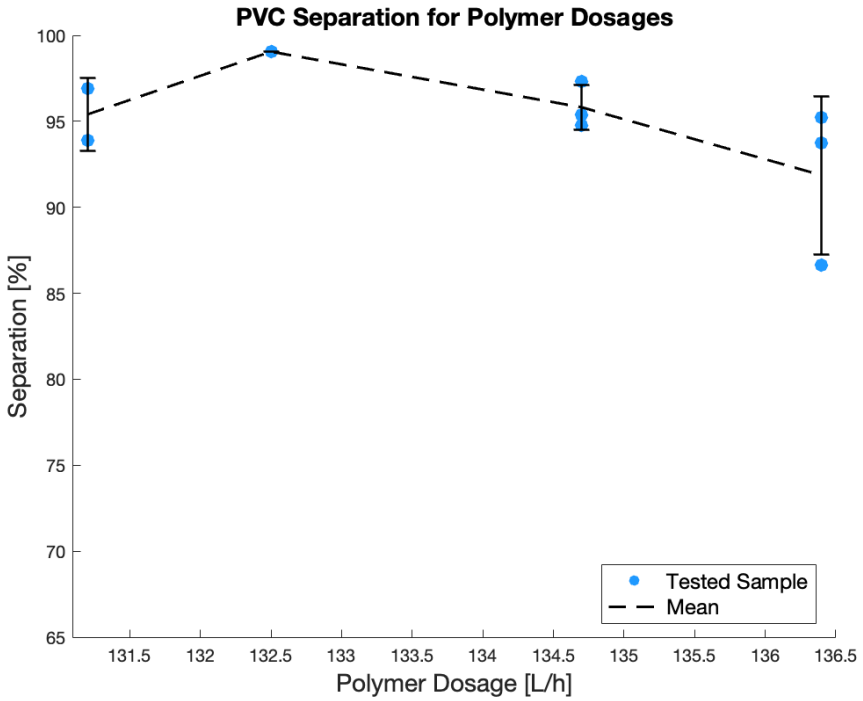

Figure 6.1: Separation in % for different dosages of polymer.

The separation efficiency of PVC in % for different polymer dosages is shown in figure 6.1, with error bars for the standard deviation and a line going through the average value for each dosage. It is clear to see that increasing the amount of polymer did not have any effect on the separation, and the deviations that were observed in separation are most likely caused by other factors. For instance, since the polymer pump is not flow compensated like the ecofloc pump, the volume fractions varied with flow rate which can explain some of the deviation in results. Due to this lack in change, it was further investigated in the CFD simulations what the minimum required dosage of flocculant would be. Total PVC waste ranged from 257.54-1703.24 g/h and a graph of this is shown in Appendix C in figure C.1.

6.1.2 Ecofloc Dosage

The same logic was applied to the ecofloc dosage study, where plotted results are those of standard size PVC production.

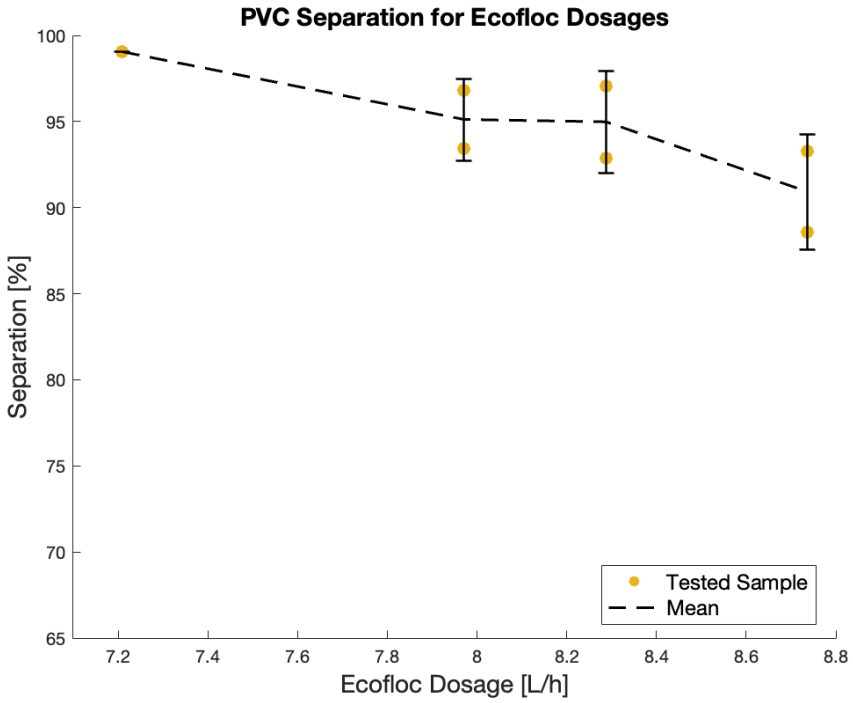

Figure 6.2: Separation in % for different dosages of ecofloc.

The separation of PVC in % for different ecofloc dosages is shown in figure 6.2 with error bars for the standard deviation and a line through the average values for each dosage. Even though it appears to be a decreasing trend with increased flocculant, it would not make sense and since the variations are very small they are likely caused by other, external factors like for the polymer dosage case. Total PVC waste ranged from 642.42-1689.81 g/h and a graph of this is shown in Appendix C in figure C.2.

6.1.3 PVC Separation for Fine Particles

More interesting results could be observed when comparing the effect of different PVC particle sizes.

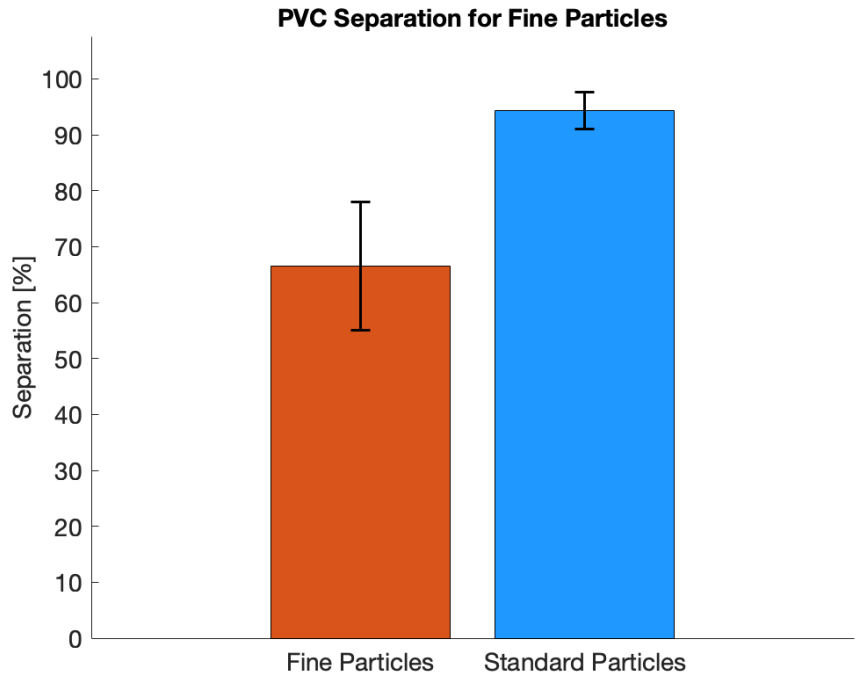

Figure 6.3: Separation in % for two different kinds of produced PVC types.

When finer PVC particles were being produced, a very drastic decline in separation could be observed as showcased in figure 6.3. The red bar with low separation includes a special type of E-PVC particles of sizes 0.5-1 μm while the blue bar with high separation consists mainly of S-PVC patricles of sizes 50-250 μm. The total PVC waste ranged from 257.54-1703.24 g/h for standard size and 2750.78-4839.54 g/h for the finer size. A graph of this is shown in Appendix C in figure C.4.

6.2 CFD simulation results

The results from the CFD simulations are first presented for the calibrated model aiming to replicate an average case, followed by results from the three case studies.

6.2.1 Calibrated Model

The resultant separation of PVC and total PVC waste found through the calibrated CFD model compared to the average values found from the laboratory experiments for standard sized particles are shown in table 6.1. Further, the flocculant consumption was found to be 70.82%.

Table 6.1: Separation efficiency for the calibrated model compared to experimental data.

Method	PVC Separation [%]	Total PVC Waste [g/h]
Calibrated CFD Model	92.33	903.54
Experimental Analysis	94.32	893.93

The slight deviation in result from the two methods was deemed insignificant, especially considering the separation from laboratory results ranged from 86.63-99.05 % and the total waste ranged from 257.54-1703.24 g/h, and the CFD results fell inbetween the minimum and maximum. In addition, velocity vectors of the flow and volume fraction contour plots of settling flocs were evaluated to calibrate the model.

6.2.1.1 Convergence Assessment

Report monitors of the volume fractions of PVC and floc product flowing from the water outlet were tracked and plotted in figure B.1, along with report monitors for the division of massflow through the two different outlets. It is clear that each of these monitors had stabilized before the 50 seconds it took for the floc product bed to stabilize.

6.2.1.2 Settling of Floc Product

The patched floc product beds by the edges of the tank sank along with the newly formed flocs towards the bottom of the tank, further filling up the cone at the bottom as shown in figure 6.4.

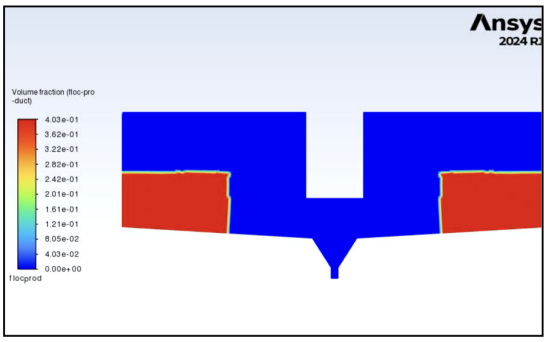

(a) t=0s.

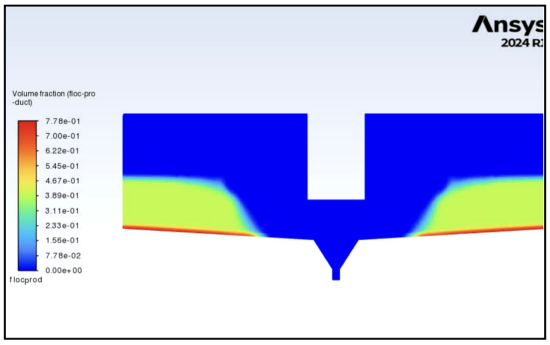

(b) t=10s.

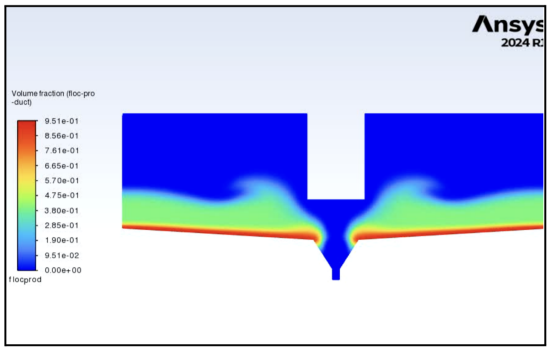

(c) t=20s.

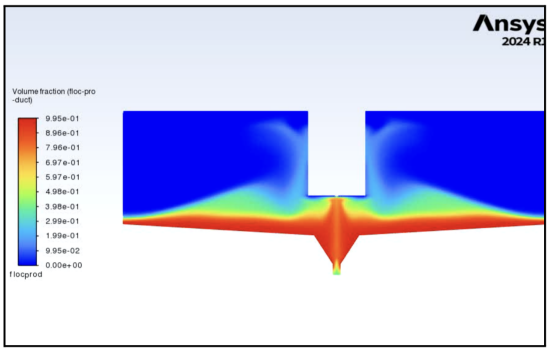

(d) t=30s.

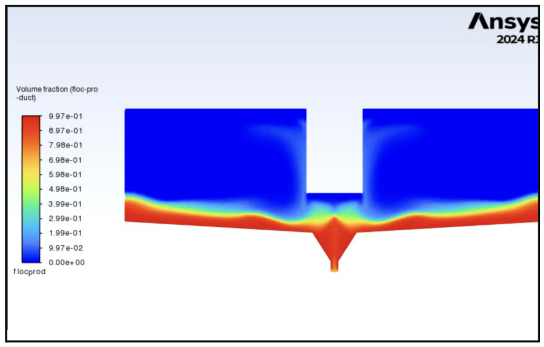

(e) t=40s.

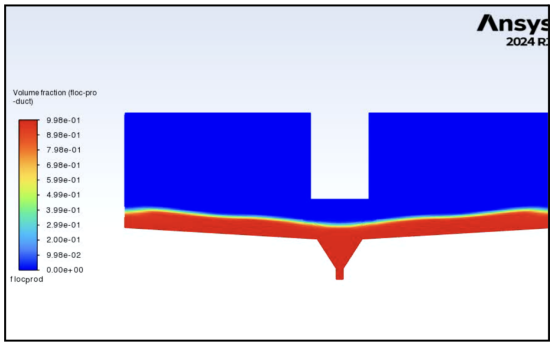

(f) t=50s

Figure 6.4: Floc product bed settling behaviour.

This behaviour explains why the flow rate from the PVC outlet of the tank is significantly lower than that of the water outlet. This bed, covering the bottom domain of the tank, stabilized after about 50 seconds.

6.2.1.3 Velocity Field Vectors

Directions of the flow field were evaluated by analyzing velocity vectors.

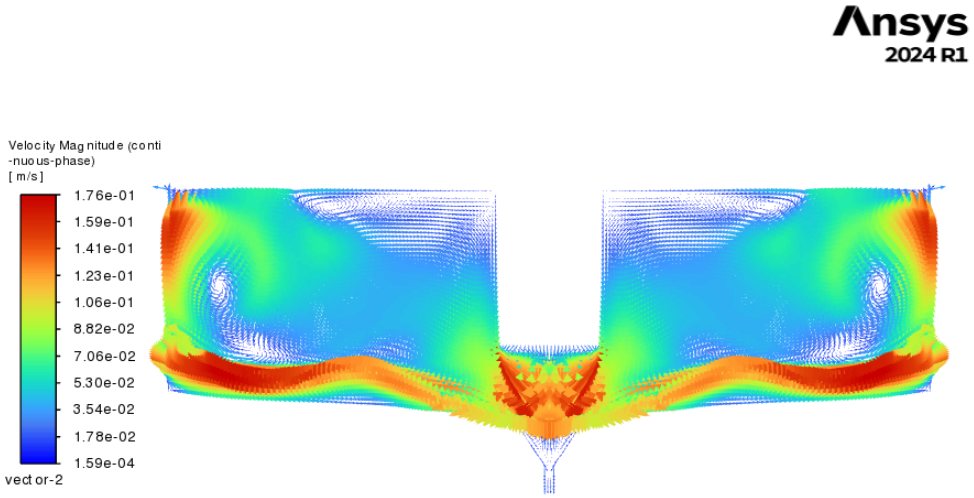

Figure 6.5: Velocity field vectors after stabilization.

In figure 6.5, vectors of velocity magnitude that ranged from 0.00016 m/s to 0.176 m/s were plotted when convergence had been reached after the floc product bed had settled. On both sides, upward flow near the walls and downward motion near the center indicate large-scale recirculation. The flow is generally slow, especially near the bottom outlet where sedimentation dominates. Some local backflow around the PVC outlet can be seen. This behavior may occur due to the low flow velocities, sediment accumulation near the outlet and the absence of a strong pressure gradient.

6.2.2 Chemical Dosage Study

The results from the Chemical Dosage Study are presented in figures 6.6 and 6.7, where each dot represents one converged simulation.

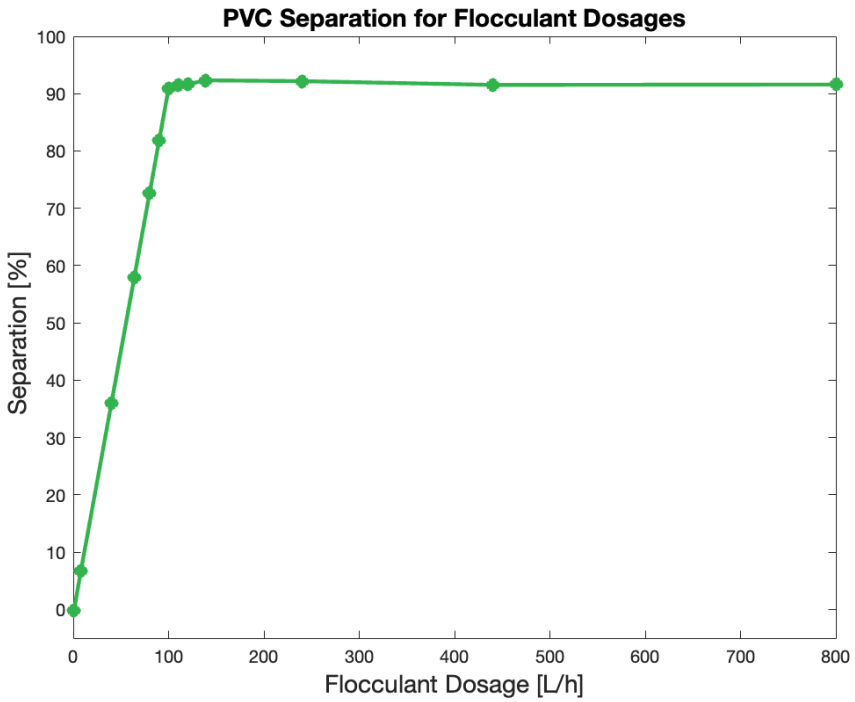

Figure 6.6: Effect of flocculant dosage on PVC separation.

The separation efficiency for different flocculant levels in the simulations behaved similarly to reality, as the entire range tested in the lab falls on the platau in figure 6.6. Since the separation does not seem to increase when the flocculant dosage exceeds a value of around 100 L/h, it is likely sufficient to decrease the flocculant dosage to this level in order to save money and use of chemicals. It is however important to note that the simulated combined flocculant does not perfectly translate to the individual amounts of required ecofloc and polymer. Total PVC waste ranged from 903.54-11865.60 g/h and a graph of this is shown in Appendix A in figure C.3.

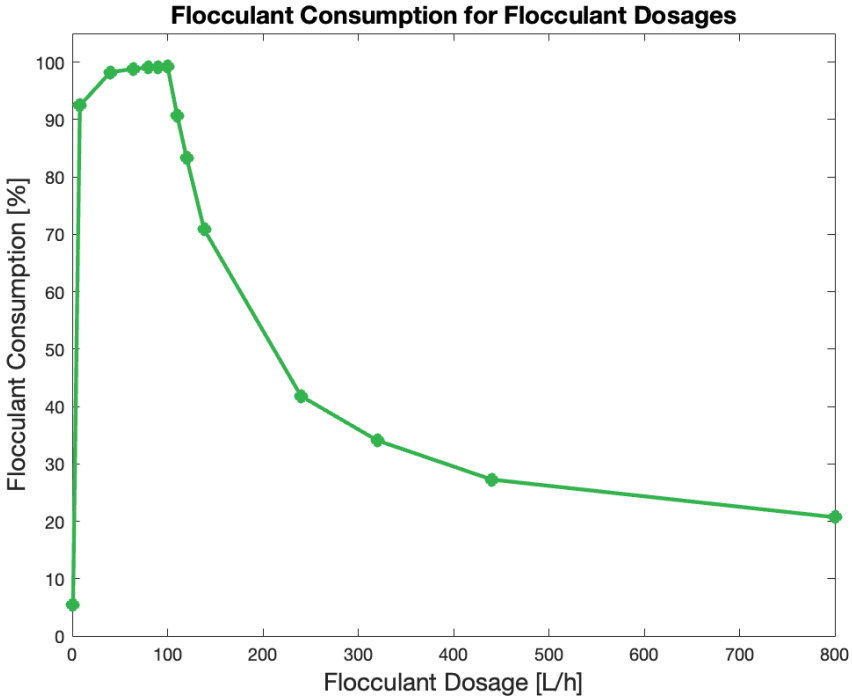

Figure 6.7: Effect of flocculant dosage on flocculant consumption.

In figure 6.7 the % of consumed flocculant is plotted, with 100% being ideal and leading to no chemical waste. It can be seen that the flocculant consumption rapidly decreases after a dosage of around 100 L/h, as the excess flocculant after this point is not able to react with the PVC. This further underlines the importance of reducing the added chemicals to a level where excess flocculant pollusion is not unnecessarily high.

6.2.3 PVC Particle Size Study

The results from the PVC Particle Size Study is presented in figure 6.8.

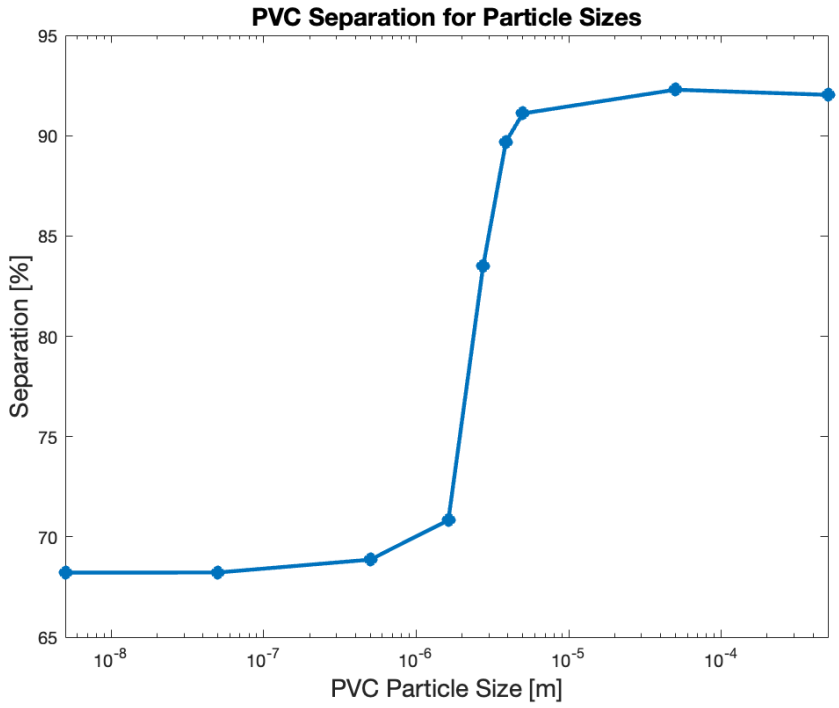

Figure 6.8: Effect of particle size on separation in logarithmic scale.

The results of the effect of varying PVC particle sizes shown in figure 6.8 are very similar to the results found in the laboratory analysis in figure 6.3. As can be seen, there is a rapid decline in separation that seems to happen when the diameter decreases from around 10 to 1 μm. Before and after that, no drastic changes can be observed. Note that the x-axis on the graph is in logarithmic scale. Total PVC waste ranged from 909.22-3533.55, g/h and a graph of this is shown in Appendix C in figure C.5. Stokes' law in equation 2.6 shows that settling velocity increases with the square of the particle diameter. This helps explain why very fine particles are significantly harder to separate in sedimentation processes.

6.2.4 PVC Production Study

The results from the PVC Production Study are presented in figures 6.9-6.11.

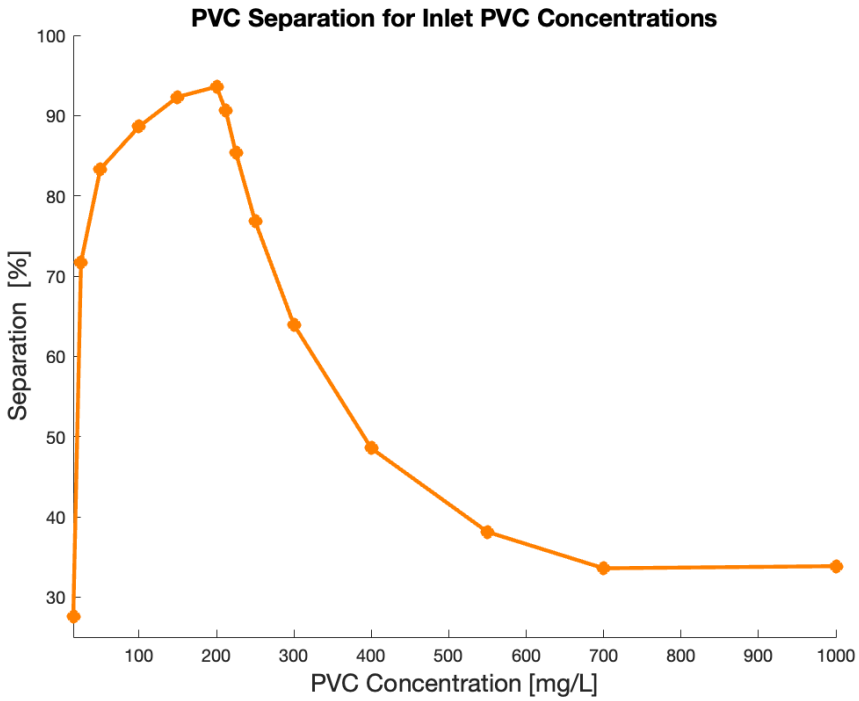

Figure 6.9: Effect of PVC inlet concentration on separation.

As shown in figure 6.9, the separation for different PVC inlet concentrations has a very distinct peak, as too low or high levels provide a drastically worse separation. At very low concentrations, particle collisions become too infrequent to support effective flocculation and at high concentrations there is not enough flocculant for the PVC to react with. The peak occured for a concentration of 200 mg/l, but a span of 125-212 also generated separation efficiencies over 90 %. Diluting the feed seems to be a promising suggestion as a strategy to keep separation levels high when inlet concentration is higher than the optimum.

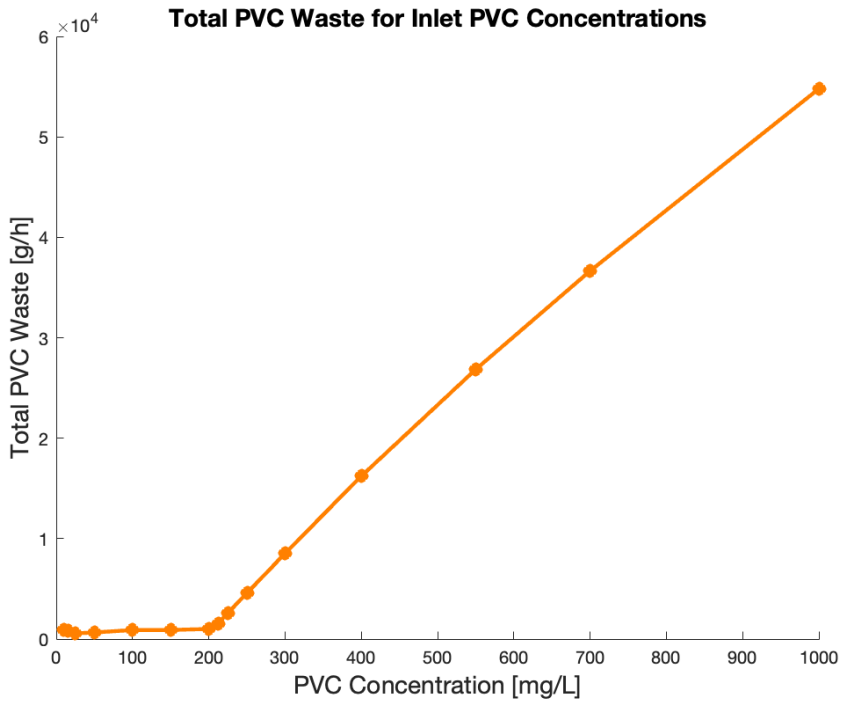

Figure 6.10: Effect of PVC inlet concentration on total PVC waste.

For values higher than 200 mg/L, the total waste output will drastically increase as the added flocculant becomes insufficient and there is excess PVC that can no longer react. This can be seen in figure 6.10. For values below 200 mg/L, the total waste output remains low due to the low input. It is important to note however, that if the concentration levels are too low, excess flocculant waste will become an issue.

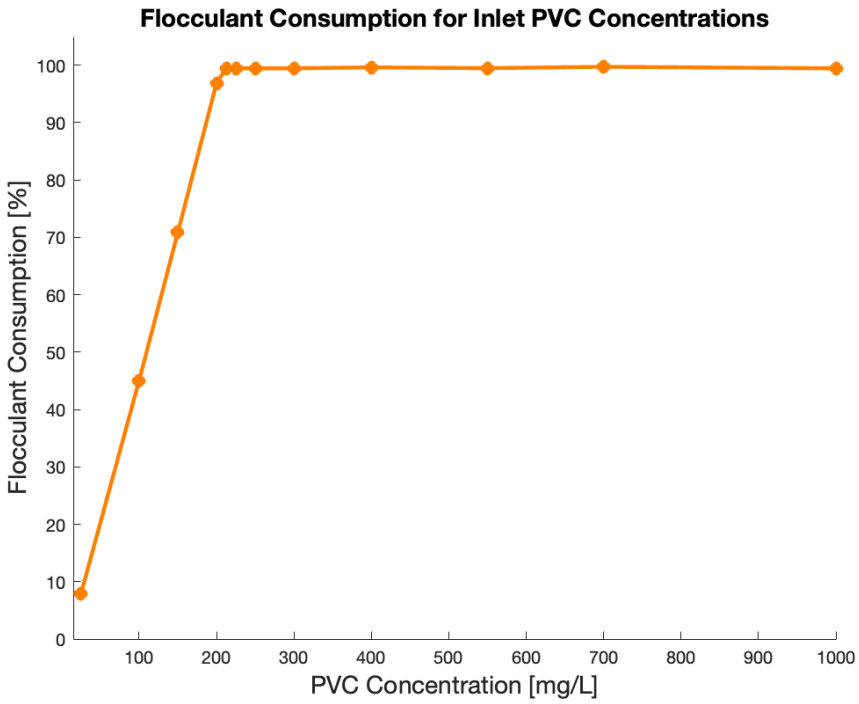

Figure 6.11: Effect of PVC inlet concentration on flocculant consumption.

As seen in figure 6.11, a PVC concentration below 200 mg/l means that excess flocculant is unable to react with the PVC, leading to large amounts of flocculant pollusion. It is therefore recommended to operate close to the peak of the separation curve. These findings do however suggest that it could be possible to decrease the concentration of PVC and added flocculant simoltaneously in order to save money on flocculant, as long as the ratio of PVC to flocculant is optimal.

6.3 Comparing CFD and Experimental Data

In order to validate the CFD results further than just comparing the calibrated model to the average real-life case, the Chemical Dosage Study and PVC Particle Size Study results could be plotted against the laborative results for further comparison.

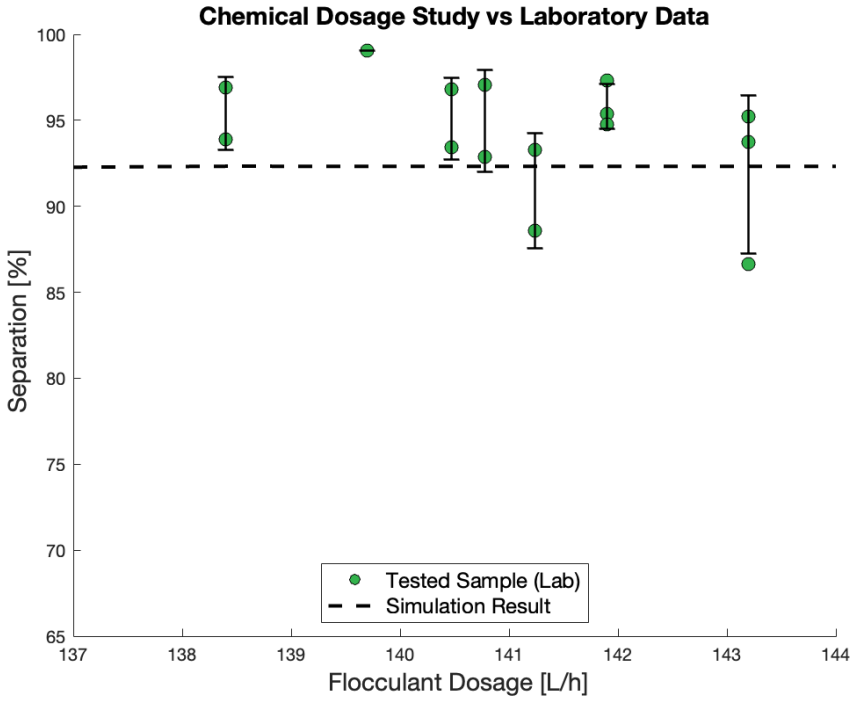

Figure 6.12: Comparing CFD and Experimental data for Chemical Dosage Study.

In figure 6.12, the separation over flocculant dosage is compared for the two methods. In the CFD simulations, results are more stable, which makes sense considering there are no other varying factors like in the real-life system where different PVC types, PVC inlet concentrations and flow rates are present. The tested laboratory samples presented in the graph represent a combination of ecofloc and polymer, like in the CFD simulations, however simply adding the two dosages in this manner provides some inaccuracy. With this in mind, the simulation follows the real-life values closely and suggests the calibrated model provides accurate results.

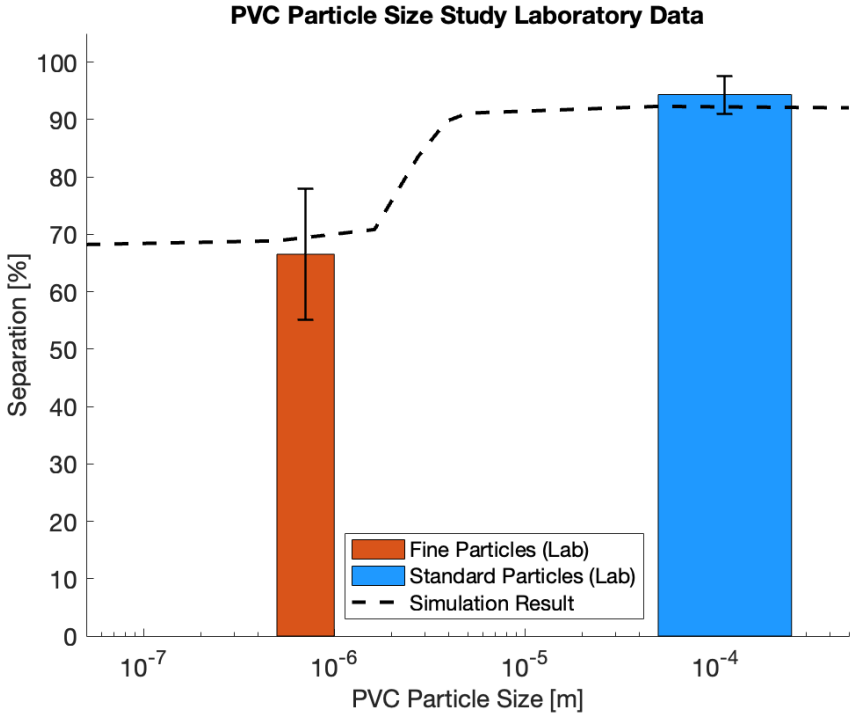

Figure 6.13: Comparing CFD and Experimental data for PVC Particle Size Study.

In figure 6.13, the separation over PVC particle size is compared for the two methods. For this case, it is even more clear to see that the CFD model provides an accurate representation of reality, considering the separation for the simulation curve aligns with the bars from experimental data. However, the size range for the two bars does not represent the entire produced distribution as multiple different PVC diameters are always present in the flow simultaneously.

6.4 Limitations of the Study

Considering the large scope of the project and the lack of available data, there are many aspects of the model that could be further improved. 3D flow effects and the rotating scrape was not accounted for, no turbulence model was applied although there is some turbulence right by the inlet and accuracy could be impproved by applying a higher-order scheme and decreasing the size of the time steps. The reaction parameters, stoichiometry, kinetics and some of the material data relied on estimations and the two flocculants were combined into one. Furthermore, perfectly spherical particles are assumed in the Euler-Euler model, which is a limitation along with the treatment of each phase as continuous. In the calibrated CFD model only one PVC particle size was applied instead of the larger distribution that is present in reality.

6.5 Industrial Application

The most important aspect to focus on henceforth would be the PVC particle size distribution, specifically the finest E-PVC types, and future research should focus on solving this issue to reduce the microplastic emissions. Efforts could further be made to keep the inflow more constant in regards to PVC concentration. A possible solution to this problem could be to add a buffer tank before the thickener tank to be able to regulate the PVC-flow. Even though a buffer tank is an expensive solution, it would be economically favorable since the biological treatment after the thickener tank is extremely expensive for the company with increasing PVC-concentrations. Moreover, if the polymer pump could be made flow compensated, the total flocculant dosage could be optimized with respect to the PVC concentration, independent of the current flow rate. This would minimize both plastic and chemical waste while saving the company money. A sufficient combined flocculant dosage was found, however no optimum was found for the polymer:ecofloc ratio which could be investigated. Rapid stirring of the flow could further serve as a way of increasing the separation efficiency in the tank. The best obtained laboratory separation of 99.05% was observed the day after the floc bed had been removed, so removing this more often could potentially help with the problem as well. There is potential that monitoring bed pressure, torque and scrape position could further prevent the need of shutting down and cleaning out the excessive floc bed.

7
Conclusion

Industrial microplastic pollution poses serious environmental and ethical concerns, as plastic waste released from chemical processes can harm marine ecosystems, contribute to climate change and threaten human health. This study addressed one aspect of that challenge by investigating how to improve the removal of PVC from industrial wastewater. This was done through combined laboratory experiments and CFD simulations. A calibrated CFD model was developed to replicate experimental results and was used to study the effects of flocculant dosage, PVC concentration, and particle size. For further research, the CFD model could be recreated using a full 3D model to also account for the effects of the rotating scrape.

The laboratory results showed no significant difference in separation performance for standard particles (50–250 μm) within the tested ranges of polymer (131–136 L/h) or ecofloc (7.2–8.7 L/h), staying between 86.63-99.05%. However, the type of PVC being produced had a substantial impact as the finer particles (0.5–1 μm) led to a drastically lower separation of only of 58.44-74.62 %. The calibrated CFD model successfully reproduced separation efficiency, total PVC waste and the settling behavior of the floc bed in the real system, and was further validated as the results from the case studies matched experimental trends.

From the Chemical Dosage Study, it was found that the current flocculant dosage lies on a plateau of peak separation performance, meaning the available PVC has already reacted and there is excess flocculant. Results indicate that the dosage could likely be reduced to 100 L/h without affecting performance, which would reduce both chemical cost and flocculant waste. This could be regulated if the polymer pump was made flow compensated and the inflow concentration was held constant. For future research, efforts could be made to try and find the optimal polymer:ecofloc ratio, as the two were treated as one in the study.

The PVC Particle Size Study showed that a sharp drop in separation efficiency occurs when PVC particle size decreases to the micrometer scale. This is likely explained by Stokes' law stating that smaller particles settle more slowly due to reduced gravitational force relative to drag, making them more difficult to flocculate. One idea to deal with this would be mixing in coarser particles into the feed during high fines content production, though this approach requires further research.

Optimal separation was achieved with an inlet concentration of 200 mg/L in the PVC Production Study. If the levels are too low, excess flocculant waste will be-

come an issue, but if they are too high, there will instead be excess PVC waste. This suggests that the process could benefit from flow regulation, either by diluting high-concentration flows by added water or by reducing flocculant dosage during low-load periods. To keep the PVC inlet concentration at an optimal, constant level, a buffer tank could potentially be installed before the thickener tank.

The thesis identifies particle size as the most critical parameter for flocculation performance. While flocculant dosage and PVC concentration appear to be near optimal under current conditions, further improvements could be achieved by focusing on the particle size distribution in the inflow, especially during production of the finest E-PVC types. Future work could investigate how to improve separation of these fine particles, either through process modifications or operational changes.

Bibliography

[1] Rahman, M. A., Mojumdar, S., Rahman, S. A., Ahmed, T., Marimuthu, K. (2023). Plastic pollutions in the ocean: their sources, causes, effects and control measures. *Journal of Biological Studies*.Available at: https://www.scopus.com/inward/record.uri?eid=2-s2.0-85171342358&partnerID=40&md5=b3dbb082a80e4efa49a82cd073326732

[2] De Frond, H. L., van Sebille, E., Parnis, J. M., Diamond, M. L., Mallos, N., Kingsbury, T., Rochman, C. M. (2019). Estimating the mass of chemicals associated with ocean plastic pollution to inform mitigation efforts. *Integrated Environmental Assessment and Management*. Available at: https://doi.org/10.1002/ieam.4147

[3] Dziak, M. (2022). Polyvinyl chloride (PVC). *Salem Press Encyclopedia of Science*. Salem Press. Available at: https://research.ebsco.com/linkprocessor/plink?id=d5b34e63-d045-313a-bd24-faa1316e5445

[4] J.J. Gallardo-Rodríguez, A. Ruiz-Ortega, E. Navarro-López, M. del C. Cerón-García, A. Sánchez-Mirón, F. García-Camacho, E. Molina-Grima (2020). Improving the learning of thickening design through graphical methods with the freeware software SMath studio. *Computer Application in Engineering Education*, *28*(6), p. 1391-1405. Available at: https://doi.org/10.1002/cae.22308.

[5] Metrohm. 930 Compact IC Flex. Available at: https://www.metrohm.com/sv_se/products/ion-chromatography/930-compact-ic-flex.html.

[6] Kamiwada, W. Y., Andrade, P. V., Reis, A. G. dos. (2020). Use of polyaluminium chloride in studies of water supply treatability through coagulation, flocculation, and sedimentation. *Engenharia Sanitária e Ambiental*, *25*(5), p. 667–676. Available at: https://doi.org/10.1590/S1413-4152202020180005

[7] Lenntech Water Treatment Solutions. (2020). BetzDearborn AE1128 – Anionic Polymeric Flocculant for Industrial Water Treatment. *SUEZ Water Technologies & Solutions Fact Sheet*. Available at: https://www.lenntech.com/Data-sheets/SUEZ-BetzDearborn-CP1157-L.pdf

[8] Lieberman, N. P., Lieberman, E. T. (2021). *Working Guide to Process Equipment* (5th ed.). McGraw-Hill Education. Available at: https://www.accessengineeringlibrary.com/content/book/9781260461664

[9] Feralco Nordic AB. (2015). *Säkerhetsdatablad: Ekoflock 50-100 6*. Available at: https://www.rskdatabasen.se/infodocs/SDB/sdb_589_5619464.pdf

[10] National Institute of Standards and Technology. *Composition of POLYVINYL CHLORIDE*. Available at: https://physics.nist.gov/cgi-bin/Star/compos.pl?ap232

[11] Andersson, B. (2012). *Computational Fluid Dynamics for Engineers*. Cambridge University Press. Available at: https://search.ebscohost.com/login.aspx?direct=true&db=cat07472a&AN=clec.DAWVLE23368033

[12] Michaelides, E. E., Sommerfeld, M., van Wachem, B. (2023). *Multiphase Flows with Droplets and Particles* (3rd ed.). CRC Press, Taylor & Francis Group. Available at: https://research.ebsco.com/c/lu54te/search/details/fekfdkfaor?limiters=FT1%3AY&q=multiphase%20flows%20of%20droplets

[13] Östlind, P. (2006). Flockning och förtjockning i High-Rate-förtjockare. Högskolan Dalarna, Akademin Industri och samhälle, Berg- och mineralteknik. Available at: https://du.diva-portal.org/smash/record.jsf?aq=%5B%5B%5D%5D&aq2=%5B%5B%5D%5D&sf=all&aqe=%5B%5D&af=%5B%5D&searchType=SIMPLE&sortOrder=author_sort_asc&onlyFullText=false&noOfRows=50&language=sv&pid=diva2%3A518071&dswid=3453

[14] Karunarathne, S. S., Tokheim, L.-A. (2017). Comparison of the Influence of Drag Models in CFD Simulation of Particle Mixing and Segregation in a Rotating Cylinder. *Linköping University Electronic Press.* p. 151–156. Available at: https://ep.liu.se/ecp/138/020/ecp17138020.pdf

[15] Grabsch, A. F., Yahyaei, M., Fawell, P. D. (2020). Number-sensitive particle size measurements for monitoring flocculation responses to different grinding conditions. *Minerals Engineering*, *145*. Available at: https://www.sciencedirect.com/science/article/abs/pii/S0892687519304996,

[16] Zare, S., Arghavani, E., Qaredaqi, M., Saedi, M. (2022). Some Opportunities to Increase Performance of Tailing Thickener: Case Study of Gol-E-Gohar Iron Ore Beneficiation Plant. *International Journal of Mining and Geo-Engineering*, *56*(1), 41–45. Available at: https://dx.doi.org/10.22059/IJMGE.2021.301280.594848

[17] ANSYS Inc. (2023). *ANSYS Fluent User's Guide* (Release 2023 R1). ANSYS Inc. Available at: https://www.ansys.com/products/fluids/ansys-fluent

[18] Peng, C., Zuo, X., Tang, C., Xu, J., Li, L. (2021). Effect of hydrophobic association on the flow behavior of partially hydrolyzed polyacrylamide solution. *AIP Advances*, *11*(6). Available at: https://pubs.aip.org/aip/adv/article/11/6/065324/995302

[19] ANSYS Inc. (2023). Pressure-Velocity Coupling. *ANSYS Fluent Theory Guide*. Available at: https://www.afs.enea.it/project/neptunius/docs/fluent/html/th/node373.htm

[20] SpringerMaterials. (2024). Water: Thermophysical Properties. Available at: https://materials.springer.com/substanceprofile/docs/smsid_uatzaqfmzswvnmaj

[21] Fatchurrohman, N., Chia, S. T. (2017). Performance of hybrid nano-micro reinforced Mg metal matrix composites brake calliper: simulation approach. *IOP Conference Series: Materials Science and Engineering*, *257*. Available at: https://doi.org/10.1088/1757-899X/257/1/012060

[22] White, D. J., Wang, J. J. (2021). Thixotropic Flocculation Effects in Carbon Black Reinforced Rubber Compounds. *Rubber Chemistry and Technology*, *94*(2), 298–312. Available at: https://meridian.allenpress.com/rct/article/94/2/298/464922

[23] Li, C., Busquets, R., Campos, L. C. (2024). Enhancing microplastic removal from natural water using coagulant aids. *Chemosphere*, *364*. Available at: https://www.sciencedirect.com/science/article/pii/S0045653524020423

[24] W. Li, M. Zhang, Q. Liu and H. Chen. (2023). Study on the Flocculation and Settling Characteristics of Anion–Cation Composite Flocculants. *Journal of Central South University (Science and Technology)*, vol. 54, no. 9, 1234-1242. Available at: https://doi.org/10.11817/j.issn.1672-7207.2023.09.020.

[25] H. Jiao, W. Chen, A. Wu, Y. Yu, Z. Ruan, R. Honaker, X. Chen, and J. Yu. (2022). Flocculated unclassified tailings settling efficiency improvement by particle collision optimization in the feedwell. *International Journal of Minerals, Metallurgy and Materials*, vol. 29, no. 12, p. 2126-2135. Available at: https://doi.org/10.1007/s12613-021-2402-3.

[26] 911 Metallurgist (2015). *Metalliferous Mining - Processing Thickening Resource Book*. Available at: https://911metallurgist.com/wp-content/uploads/2015/08/thickening-basics.pdf.

[27] H.G. Merkus (2009). Sedimentation techniques. *Particle Size Measurements: Fundamentals, Practice, Quality*, Springer, p. 319-348. Available at:.

A

CAD Model of the Thickener Tank

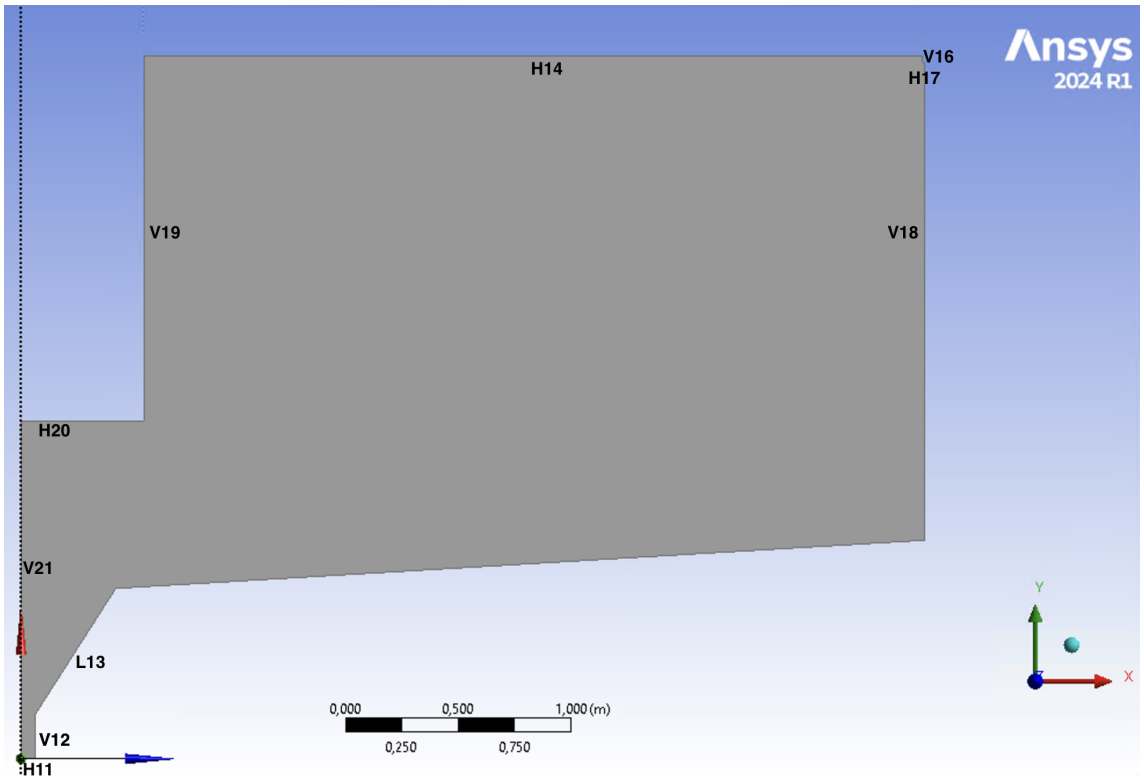

Figure A.1: CAD-Sketch of the 2D axisymmetric thickener tank.

Table A.1: CAD model dimensions.

Side	Dimension [m]
H11	0,065
H14	3,454
H17	0,01
H20	0,545
L13	0,66
V12	0,2
V16	0,03
V18	2,12
V19	1,62
V21	1,5

B

CFD Convergence Monitors

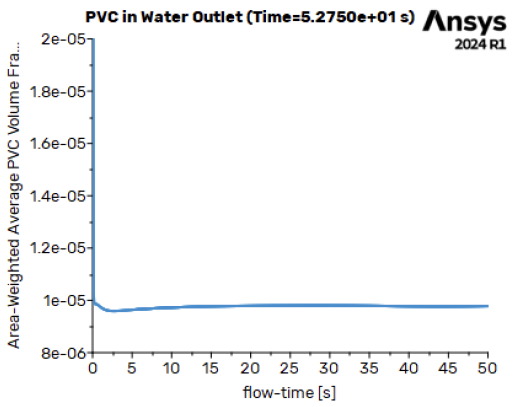

(a) Volume fraction of PVC in water outlet

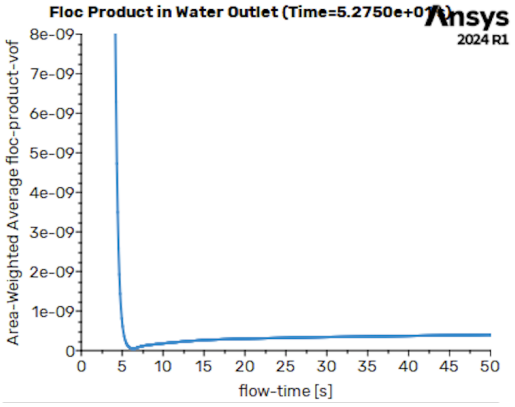

(b) Volume fraction of floc product in water outlet.

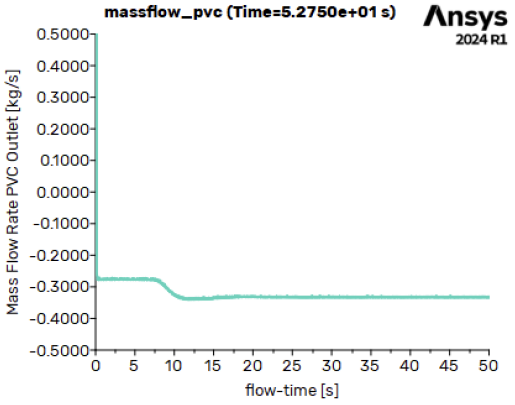

(c) Total mass flow from PVC outlet.

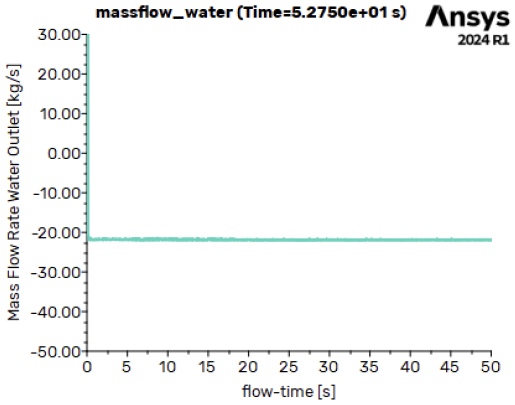

(d) Total mass flow from water outlet.

Figure B.1: Convergence monitors for calibrated model.

C

Total PVC Waste Data

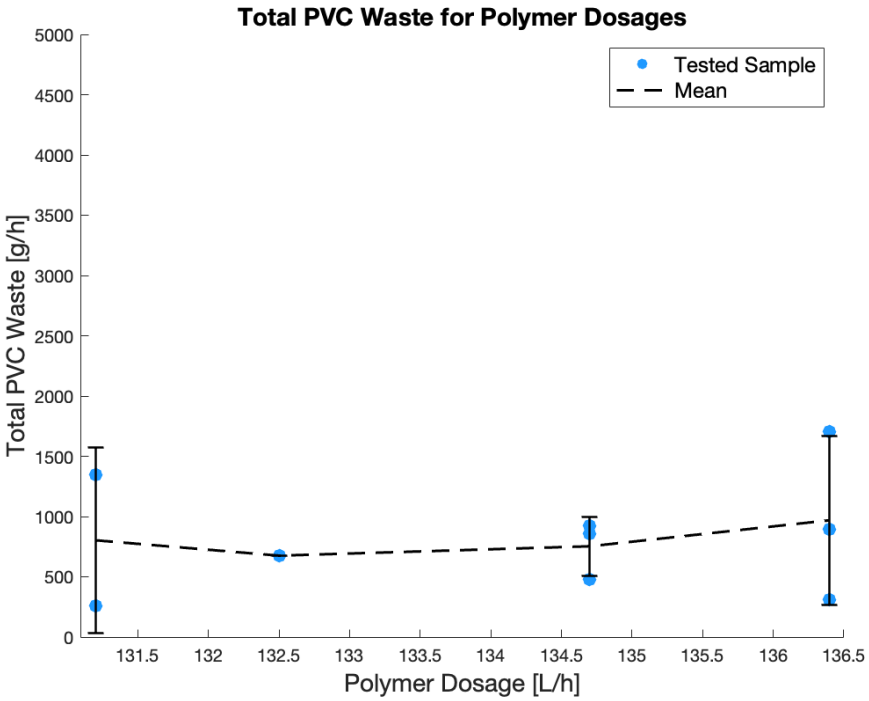

Figure C.1: Total Waste for different dosages of polymer from laboratory analysis.

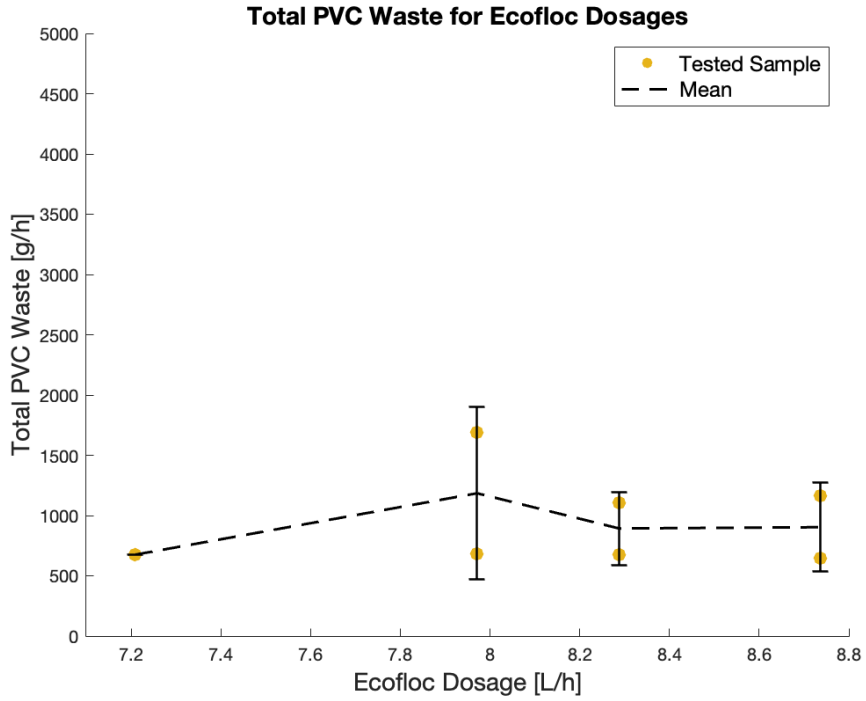

Figure C.2: Total Waste for different dosages of Ecofloc from laboratory analysis.

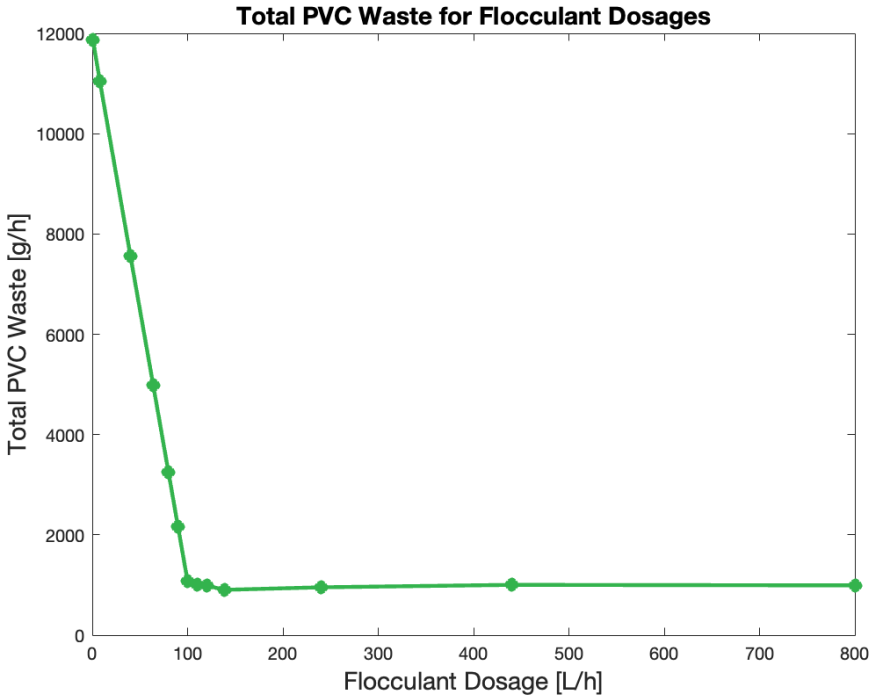

Figure C.3: Total Waste for different dosages of flocculant from CFD simulation.

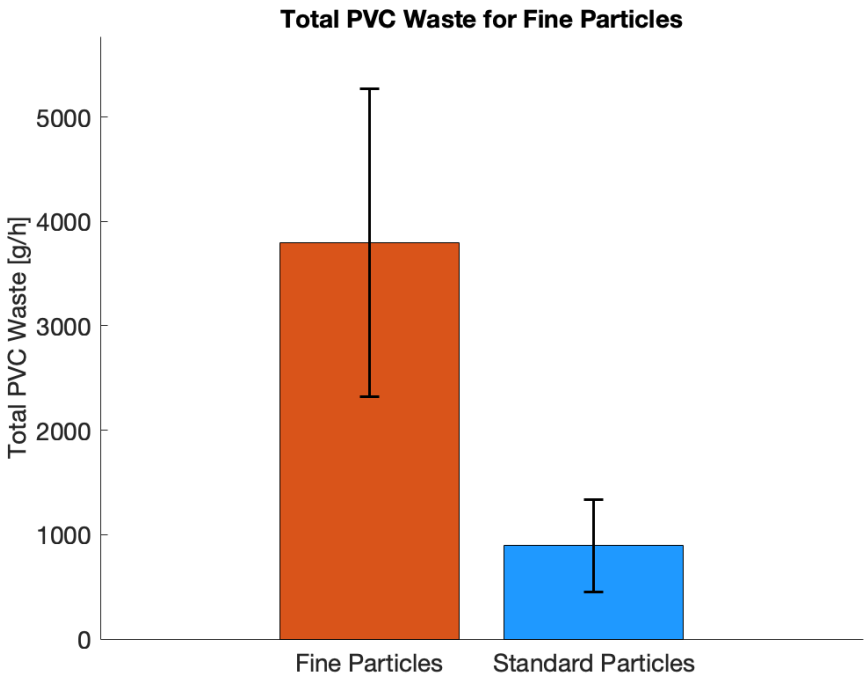

Figure C.4: Total Waste for different PVC particle sizes from laboratory analysis.

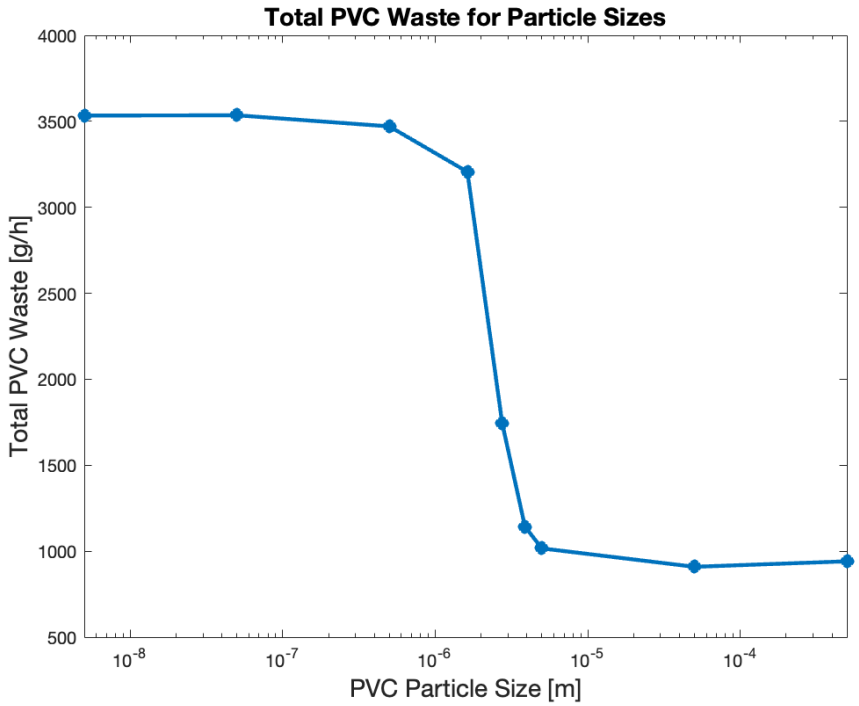

Figure C.5: Total Waste for different PVC particle sizes from CFD simulation.

DEPARTMENT OF MECHANICS AND MARITIME SCIENCES
CHALMERS UNIVERSITY OF TECHNOLOGY
Gothenburg, Sweden 2025
www.chalmers.se

CHALMERS
UNIVERSITY OF TECHNOLOGY